Aus der Medizinische Klinik und Poliklinik IV
Klinik der Universität München
Direktor: Prof. Dr. Martin Reincke

Using TGF-β1 Biology in Radioiodine Refractory Differentiated Thyroid Cancer to Re-establish Sodium Iodide Symporter (NIS) Expression Using Engineered Mesenchymal Stem Cells as Therapy Vehicles

Dissertation
zum Erwerb des Doktorgrades der Medizin
an der Medizinischen Fakultät der
Ludwig-Maximilians-Universität zu München

vorgelegt von

Yang Han

aus

Zhengzhou, Henan, China

2023

Mit Genehmigung der Medizinischen Fakultät
der Universität München

Berichterstatter: Prof. Dr. Christine Spitzweg

Mitberichterstatter: Prof. Olivier Gires
                                     PD Dr. Vera Wenter
                                     Prof. Dr. Horst Zitzelsberger

Mitbetreuung durch den

promovierten Mitarbeiter: Prof. Dr. Peter Jon Nelson

Dekan: Prof. Dr. med. Thomas Gudermann

Tag der mündlichen Prüfung: 26.01.2023

Affidavit

LMU LUDWIG-MAXIMILIANS-UNIVERSITÄT MÜNCHEN	Promotionsbüro Medizinische Fakultät	MMRS	

Affidavit

Han, Yang
_____
Surname, first name

_____
Street

450000, Zhengzhou, China
_____
Zip code, town, country

I hereby declare, that the submitted thesis entitled:

Using TGF-β1 Biology in Radioiodine Refractory Differentiated Thyroid Cancer to Re-establish Sodium Iodide Symporter (NIS) Expression Using Engineered Mesenchymal Stem Cells as Therapy Vehicles.

is my own work. I have only used the sources indicated and have not made unauthorised use of services of a third party. Where the work of others has been quoted or reproduced, the source is always given.

I further declare that the dissertation presented here has not been submitted in the same or similar form to any other institution for the purpose of obtaining an academic degree.

Zhengzhou, 13.02.2023
_____
place, date

Yang Han
_____
Signature doctoral candidate

1. Table of content

2. Summary

Based on its role in mediating iodide uptake from the blood into the thyroid, the sodium iodide symporter (NIS) allows radioiodine imaging and therapy of differentiated thyroid cancer. This biology is largely responsible for the favorable prognosis of most thyroid cancers. However, due to the loss of functional NIS expression, a number of thyroid cancers remain refractory to radioiodine (RAI) including RAI-refractory differentiated thyroid cancer (DTC) and anaplastic thyroid cancer (ATC). The delivery of *NIS* as a transgene into refractory tumors represents a therapeutic strategy for RAI-refractory thyroid cancer and metastasis. Previous studies have extensively investigated the transfer of the NIS gene into experimental tumor models using viruses, polymers or mesenchymal stem cells (MSCs) as delivery vehicles. MSCs are under development for *NIS* gene transfer based on their excellent tumor homing abilities. In this regard, various strategies have been applied to enhance the tumor-specificity and effectiveness of MSC-mediated NIS gene transfer.

Based on the critical role of Transforming growth factor beta (TGF-β) in thyroid cancer including driving tumor-directed migration of MSCs, and the identification of an autocrine TGF-β loop as a mechanism through which BRAFV600E fosters NIS repression, in the present thesis we proposed to re-induce NIS-mediated radioiodine uptake in tumor mouse models using a synthetic TGF-β1-inducible/SMAD-responsive promoter in engineered MSCs (SMAD-NIS-MSCs) to drive NIS expression. As the first step, TGF-β levels were evaluated in different thyroid cancer cell lines by qRT-PCR and ELISA. Tumor cell-conditioned medium was then used to evaluate stimulation of NIS expression in SMAD-NIS-MSCs. In parallel experiments validation of TGF-β induced NIS expression in SMAD-NIS-MSCs was studied through co-culture of the thyroid cancer cells with the engineered MSCs. SMAD-NIS-MSCs demonstrated different levels of radioiodine uptake after stimulation with either tumor conditioned medium or by co-culture with thyroid cancer cells.

A 3D live chemotaxis assay confirmed the directed migration of MSCs towards supernatants derived from K1 and BCPAP papillary thyroid cancer (PTC) cells as compared to control culture medium. This tumor directed migration of MSCs was further validated *in vivo* using K1 and BCPAP xenograft mouse models. Systemic injection of SMAD-NIS-MSCs showed effective tumor homing of the cells with functional NIS gene transfer resulting in a high level of tumoral radioiodine uptake in both subcutaneous tumor models as compared to WT-MSCs analyzed by ^{123}I-scintigraphy. Tumor-specific NIS expression in tumor bearing mice treated with SMAD-NIS-MSCs was further confirmed *ex vivo* by NIS immunohistochemistry. A therapy study of the experimental tumors using systemically administered SMAD-NIS-MSCs followed by ^{131}I treatment resulted in a significantly prolonged survival with reduced tumor growth in the therapy groups in both animal models. Immunofluorescence analysis of Ki67 and CD31 expression in the resected tumors demonstrated a decrease in tumor proliferation index and blood vessel density in therapy mice.

Taken together, the work presented in this thesis support the exciting prospect of using NIS-mediated radioiodine therapy for the treatment of RAI refractory thyroid tumors by taking advantage of the tumor-selective homing of MSCs and targeting the TGF-β biology in RAI refractory thyroid cancer. We were able to hit the tumor with its own weapons by targeting the TGF-β/SMAD signaling to re-induce radioiodine accumulation in the tumor stroma and make use of the crossfire effect of ^{131}I to achieve effective therapy.

3. Zusammenfassung

Der Natrium-Iodid-Symporter (NIS) ist an der basolateralen Membran der Schilddrüsenfollikelzellen lokalisiert und vermittelt dort die aktive Iodid-Aufnahme. Er ist die molekulare Basis für die Radioiod-Diagnostik und -Therapie beim differenzierten Schilddrüsenkarzinom und stellt damit eines der ältesten und erfolgreichsten Targets für molekulare Bildgebung und molekular gezielte Radionuklidtherapie dar. Diese Biologie trägt maßgeblich zu einer günstigen Prognose der differenzierten Schilddrüsenkarzinome bei.

Aufgrund eines Verlusts der Expression und/oder einer defekten Membran-Verankerung des NIS zeigt ein Teil der Schilddrüsenkarzinome ein Radioiod (RAI)-refraktäresVerhalten, dazu zählen die RAI-refraktären differenzierten (DTC) sowie die anaplastischen Schilddrüsenkarzinome (ATC). Der Transfer von NIS als Transgen in RAI-refraktäre Tumore stellt eine therapeutische Strategie für entsprechende Schilddrüsenkarzinome und deren Metastasen dar. Frühere Studien, einschließlich der Vorarbeiten unserer Arbeitsgruppe, haben den Transfer des NIS-Gens in experimentelle Tumormodelle unter Verwendung verschiedener Transportvehikel wie beispielsweise Viren, Polymere oder mesenchymalen Stammzellen (MSCs) ausführlich untersucht.

MSCs stellen vielversprechende tumorselektive Gentransfervehikel dar, da sie aufgrund ihres intrinsischen „Tumor Homings" die Eigenschaft besitzen, gezielt in das Tumorgewebe zu migrieren, und können daher nach genetischem Engineering wie ein trojanisches Pferd genutzt werden, um therapeutische Gene im Tumor gezielt zu exprimieren. Diese Eigenschaften erlauben eine stabile Transfektion der MSCs mit dem theranostischen NIS-Gen, um dieses gezielt in das Tumorstroma zu transportieren und dort zu exprimieren. F r die Verwendung von MSCs als Gentransfervehikel in der Tumortherapie sind Promotoren zur Kontrolle der Expression des therapeutischen Gens vorteilhaft, welche spezifisch im Tumorstroma aktiviert werden. Durch die Promoter-kontrollierte Aktivierung des NIS-Gens im

Tumormikromilieu kann eine Erhöhung der Selektivität der Genexpression im Tumorgewebe mit Minimierung der systemischen Nebenwirkungen erreicht werden.

Basierend auf der zentralen Rolle von Transforming Growth Factor β (TGF-β) in der Pathogenese von Schilddrüsenkarzinomen insbesondere bei der BRAFV600E-induzierten Repression der NIS Expression in BRAFV600E-positiven papillären Schilddrüsenkarzinomen, soll in der vorliegenden Arbeit unter Verwendung eines synthetischen TGF-β1-induzierbaren/SMAD-responsiven Promoters zur Steuerung der NIS Expression in gentechnisch veränderten MSCs (SMAD-NIS-MSCs), die Re-Induktion einer NIS-vermittelte Radioiodaufnahme *in vivo* im Schilddrüsenkarzinom-Mausmodell untersucht werden.

In einem ersten Schritt wurde der TGF-β-Spiegel in verschiedenen Schilddrüsenkarzinomzelllinien durch qRT-PCR und ELISA. Des Weiteren wurde Tumorzell-konditioniertes Medium verwendet, um die Stimulation der NIS-Expression in SMAD-NIS-MSCs zu evaluieren. In parallelen Experimenten wurde die Validierung der TGF-β-induzierten NIS-Expression in SMAD-NIS-MSCs durch Co-Kultivierung der gentechnisch modifizierten MSCs mit Schilddrüsenkarzinomzellen untersucht. SMAD-NIS-MSCs zeigten nach Stimulierung entweder mit tumorzellkonditioniertem Medium oder durch Co-Kultur mit Schilddrüsenkarzinomzelllinien unterschiedlich hohe Radioiodaufnahme Level.

Ein 3D-Live-Chemotaxis-Assay bestätigte im Vergleich zum Kontrollkulturmedium die gerichtete Migration von MSCs zu Überständen, die von den papillären Schilddrüsenkarzinomzelllinien K1- und BCPAP stammten. Des Weiteren wurde diese tumorgerichtete Migration von MSCs *in vivo* unter Verwendung von K1- und BCPAP-Xenotransplantat-Mausmodellen validiert. Die systemische Injektion von SMAD-NIS-MSCs zeigte ein effektives „Tumor-Homing" der MSCs mit funktionellem NIS-Gentransfer, was durch eine hohe tumorale Radioiodaufnahme bei der ^{123}I-Szintigraphie in beiden subkutanen Tumormodellen im Vergleich zur Kontrolle mit Wildtyp (WT)-MSCs führte. Die tumorspezifische NIS-Expression in Tumor-tragenden Mäusen, die mit SMAD-NIS-MSCs behandelt wurden, konnte *ex vivo* durch NIS-

Immunohistochemie bestätigt werden. Therapiestudien in beiden Schilddrüsenkarzinomzell-Xenograft-Mausmodellen, in welchen SMAD-NIS-MSCs systemisch verabreicht wurden, gefolgt von einer ^{131}I-Behandlung, zeigten ein signifikant verlängertes Überleben bei reduziertem Tumorwachstum in den Therapiegruppen. Die Immunfluoreszenzanalyse der Ki67- und CD31-Expression in den resezierten Tumoren zeigte eine Abnahme des Tumorproliferationsindex und der Blutgefäßdichte bei Therapiemäusen.

Durch Instrumentalisierung des aktivierten TGF-β/SMAD-Signalwegs in Radioiod-refraktären Schilddrüsenkarzinomen konnte unter Verwendung der SMAD-NIS-MSCs die tumorale NIS-Expression re-induziert werden und der Tumor durch den Crossfire-Effekt der ^{131}I-Therapie sozusagen „mit seinen eigenen Waffen" geschlagen werden.

Die Ergebnisse dieser Arbeit zeigen das große Potenzial einer MSC-vermittelten, TGF-β1-induzierten, NIS-basierten ^{131}I-Therapie als eine neue, innovative Therapiestrategie zur Behandlung Radioiod-refraktärer Schilddrüsenkarzinome.

4. Abbreviations

AFP	alpha-fetoprotein
ATC	anaplastic thyroid cancer
Camp	cyclic adenosine monophosphate
CEA	carcinoembryonic antigen
CM	conditioned medium
CMV	cytomegalovirus
CoM	center-of-mass
DMEM	Dulbecco's Modified Eagle Medium
DTC	differentiated thyroid cancer
EGFR	epidermal growth factor receptor
ELISA	enzyme-linked immunosorbent assay
EMT	epithelial‑to‑mesenchymal transition
FBS	fetal bovine serum
FMI	forward migration index
GCV	ganciclovir
HCC	hepatocellular carcinoma
HSV	herpes simplex virus
i.p.	intraperitoneal
i.v.	intravenous
IFN-β	β-interferon
IL-2	interleukin-2
LPEI	linear polyethylenimine

LPS	lipopolysaccharide
MAPK	mitogen-activated protein kinase
MHCII	major histocompatibility complex type II
MSC	mesenchymal stem cells
MTC	medullary thyroid carcinoma
MV	measles virus
NF-κB	nuclear factor-Kb
NIS	sodium iodide symporter
NUE	NIS upstream enhancer
OEI	oligoethylenimine
PDTC	poorly differentiated thyroid cancer
PEG	polyethylene glycol
PET	positron emission tomography
PMA	phorbol-myristate-acetate
Poly-HEMA	Poly 2-hydroxyethyl methacrylate
PSA	prostate specific antigen
PTC	papillary thyroid cancer
qRT-PCR	quantitative real-time polymerase chain reaction
RAI	radioiodine
ROI	regions of interest
SPECT	single photon emission computed tomography
TG	thyroglobulin
TGF-β	transforming growth factor-beta
TNF-α	tumor-necrosis-factor-α

TPO   thyroid peroxidase

TRAIL   tumor necrosis factor-α-related apoptosis-inducing ligand

TSH   thyroid-stimulating hormone

VEGF   vascular endothelial growth factor

VV   vaccinia virus

WT   wild-type

5. Introduction

5.1 Thyroid Cancer – an overview

Cancer is deemed to be a leading cause of death, accounting for an estimated 19.3 million new cases and 10 million deaths all over the world in 2020 [1]. The incidence and mortality of cancer is growing despite early detection through enhanced screening programs and a series of breakthroughs in treatment in the last few decades. Thyroid cancer, the most common endocrine malignancy, is ranked ninth in incidence, and accounts for roughly 3% of total estimated new cancer cases [2, 3]. Although the majority of thyroid cancers are treatable, radioiodine refractory differentiated thyroid cancer, dedifferentiated thyroid cancers including poorly differentiated and anaplastic thyroid cancers remain a therapeutic challenge and are still almost uniformly lethal. This highlights the need for novel treatment options for these advanced thyroid cancers.

The main histologic subtypes of thyroid carcinoma are differentiated thyroid carcinoma (DTC; including papillary thyroid cancer (PTC) and follicular thyroid cancer (FTC)), poorly differentiated thyroid cancer (PDTC), anaplastic thyroid carcinoma (ATC) and medullary thyroid carcinoma (MTC). Among these subtypes, PTC, FTC, PDTC and ATC arise from thyroid follicular cells, while MTC represents a canonical C-cell tumor with different biologic features [4]. For this study, we focused on cancers that origin from follicular cells.

5.2 Molecular basis

Carcinogenesis is a complex process. Cells evolve progressively towards malignant cells via a series of steps, where they acquire the abilities of sustained proliferation, circumvention of growth suppressors, eluding cell death, replicative immortality, evasion of the immune system, readjustment of energy metabolism, induction of angiogenesis, and the ability to invade surrounding tissues and form metastases in other organs [5, 6]. Additionally, two consequential characteristics were thought to help

promote carcinogenesis: genomic instability and mutation, and tumor-promoting inflammation [6]. In the context of thyroid cancer, different molecular alterations are thought to be associated with specific stages of the multistep-tumorigenic process.

The development of PTC, which accounts for the majority (~85%) of thyroid cancers, is largely caused by the *BRAF* V600E (60%) mutation, followed by *RAS* (15%) mutations, and chromosomal rearrangements such as seen with *RET/PTC* (12%) [4]. FTC and follicular variants of PTC are linked to mutually exclusive mutations of *RAS* or the PAX8–PPARG rearrangement. PDTC and ATC, although *BRAF* and *RAS* are predominant drivers, are also characterized by *TERT* promoter mutations, *TP53* inactivation and dysregulation of the PI3K–PTEN–AKT pathway [7]. These genetic changes are strong inducers of dedifferentiation and linked to invasion and progression.

BRAF is a serine-threonine kinase linked to the RAS-RAF-MAPK kinase signaling pathway that promotes cell proliferation and mobility. The most common mutation of the BRAF gene, BRAF V600E, is a thymine to adenine substitution at nucleotide position 1799, that results in a valine-to-glutamate acid substitution at residue 600 (Val600Glu). This mutation strongly enhances BRAF kinase activity eliciting phosphorylation activity on the downstream extracellular-signal-regulated kinase (ERK)1/2, leading to alterations in the expression of various genes involved in tumorigenesis [8, 9].

Human *RAS* including *HRAS*, *KRAS* and *NRAS* encode G-proteins located on the cell membrane that also mediate signal transduction in the RAS-RAF-MAPK kinase signaling and PI3K–AKT pathways. NRAS codon 61 mutation is common in thyroid cancers, and mainly present in FTC, PDTC, ATC and in follicular variants of PTC [7]. Mutations in RAS typically inhibit the GTPase activity and lock the protein in the active GTP bound form, that is associated with increased aggressiveness and decreased survival in patients [10, 11].

RET is a proto-oncogene that encodes the cellular tyrosine kinase transmembrane receptor that binds the neurotrophic factor ligand, forming a cell surface complex that activates downstream signaling, including MAPK pathways. Chromosomal

rearrangement of *RET* can be caused by exposure to ionizing radiation, resulting in fusion of the *RET* tyrosine kinase domain with the partner genes such as *CCDC6* or the nuclear receptor co-activator 4 gene (*NCOA4*), leading to uncontrolled stimulation of MAPK pathways, thus increasing the proliferation of the follicular cells and enhanced malignancy [12].

The MAPK signaling pathway plays a key role in thyroid cancer by regulating cell proliferation and promoting the dedifferentiation particularly in PTC. Activation of MAPK promotes the release of key factors such as TSP1, TGF-β1, VEGF, matrix proteins and MMPs all linked to tumor progression and metastasis [13]. MAPK activation is also thought to be the main driver of suppression or reduced sodium iodide symporter (NIS) expression as well as other thyroid specific genes [14].

5.3 The sodium iodide symporter (NIS)

5.3.1 Basic characteristics

NIS is an intrinsic transmembrane glycoprotein that is found in the thyroid follicular cells' basolateral membrane and facilitates the uptake of iodide into the thyroid gland and other extrathyroidal organs. Two ions of sodium (Na^+) and one of iodide (I^-) are transported into the cells and the process relies upon the Na^+ gradient maintained by Na^+/K^+ ATPase [14]. In addition to I^- transport, other anions are transported by NIS albeit with less efficiency including: selenium cyanate ($SeCN^-$), thiocyanate (SCN^-), chlorate (ClO_3^-) and nitrate (NO_3^-) [15]. Another anion, perchlorate (ClO_4^-), inhibits I^- transport in a competitive manner. These physiologic characteristics of NIS offer the molecular foundation for diagnostic imaging and treatment of thyroid cancer and its metastases using radionuclides transported by NIS.

5.3.2 *NIS* as theranostic gene

The first therapeutic use of radioiodine (RAI) was in a patient with hyperthyroidism in 1941. 5 years later, RAI was successfully used to diagnose and treat thyroid carcinoma by Saul Hertz [16]. The gene responsible for thyroidal RAI uptake, *NIS*, was cloned

and characterized by Nancy Carrasco in 1996, allowing the development of a *NIS* cytoreductive gene therapy strategy combined with NIS multimodal imaging in thyroidal and non-thyroidal tumors [17]. *NIS* had been used for radionuclide imaging of thyroid cancers and metastases, by non-invasive scintigraphy (^{123}I or ^{99m}Tc), single photon emission computed tomography (SPECT) (^{125}I, ^{99m}Tc or ^{188}Re), or by positron emission tomography (PET) imaging (^{124}I or ^{18}F-TFB) [18]. The diagnostic use of radionuclides for NIS imaging allows tumor-absorbed dosimetry before therapeutic application of ^{131}I, ^{188}Re or ^{211}At to help determine the appropriate dose [19]. The therapeutic effect of radionuclides is achieved by ionization, which leads to the damage of cellular proteins and DNA breaks. A further characteristic of NIS-mediated radioiodine treatment is the bystander effect, which is caused by a crossfire effect of the β-emitting ^{131}I with a path length of 2.4 mm and resulting in the cellular apoptosis of neighboring cells [20]. In addition, the radioiodine is oxidized with the catalyzation of thyroid peroxidase (TPO) followed by incorporation of iodide into the backbone of the thyroglobulin (TG) in thyroid follicular cancer cells, which is called iodide organification, causing a prolonged retention time of tumoral iodine resulting in a high dose of ^{131}I absorbed by the tumors [21].

5.3.3 Regulation of NIS

Although radioactive iodine treatment has been successfully used in thyroid cancer patients, some tumors exhibit recurrence and distant metastases because of the loss of the ability to accumulate ^{131}I either from the very beginning or gradually over time, which is termed RAI-refractory thyroid cancer [22]. The main reason for RAI-refractoriness is a decreased expression of functional NIS or a diminished targeting of NIS to the plasma membrane, or both [13].

In the thyroid NIS expression is regulated by the thyroid-stimulating hormone (TSH). Stimulation by TSH activates adenylyl cyclase through a Gs-protein, resulting in elevation of endogenous cyclic adenosine monophosphate (cAMP). Activated cAMP stimulates NIS expression by binding to the NIS upstream enhancer (NUE) via the

paired box 8 (PAX8) through both protein kinase-A (PKA)-dependent and PKA-independent pathways [21-24].

In thyroid cancers, aberrant activation of the MAPK pathway is considered to play a major role in NIS repression, that is mainly driven by the oncogene *BRAF V600E*, *RET/PTC* rearrangements or *RAS* mutation [13]. The oncoproteins encoded by these altered genes especially *BRAF V600E* constitutively activate the downstream ERK1/2, resulting in the loss of expression of NIS and other iodide-metabolizing genes [25]. This loss of NIS expression partially relies on transforming growth factor-beta (TGF-β) signaling. The TGF-β family of cytokines act as tumor suppressors in early stages of tumor progression, but can also help drive tumor initiation, progression and metastasis, as well as contribute to epithelial‑to‑mesenchymal transition (EMT) in advanced cancers [26-29]. The oncogene *BRAF V600E* is a strong inducer of TGF-β in thyroid malignancies, and TGFβ decreases NIS expression by reducing TSH transcriptional activation [27, 30-32]. TGF-β downregulates PAX8 through activation of SMAD3 and evokes an inhibition of PAX8 binding to the NIS promoter. Furthermore, TGF-β induces the activation of ERK in a SMAD-independent manner [33]. In addition, BRAF-induced TGF-β delocalizes NIS from the plasma membrane leading to the loss of iodide uptake [14].

The PI3K/AKT signaling pathway also plays a fundamental role in the progression of thyroid cancer and has been shown to suppress NIS and other iodide-metabolizing genes [34-36]. In normal thyroid cells, IGF1 can repress TSH-induced transcription of NIS, and this effect can be blocked by the PI3K inhibitor LY294002 demonstrating that IGF1 can mediate repression of NIS expression through the PI3K/AKT signaling pathway [35]. Inhibition of AKT, which is downstream of PI3K, results in post-translational stimulation of NIS and increased iodide uptake in some thyroid cancer cells [36]. In addition, activation of mTOR, downstream of the PI3K/AKT signaling pathway, has also been implicated in a decrease in NIS expression and RAI resistance [37].

The nuclear factor Nuclear factor-κB (NF-κB) pathway is also linked to the regulation of *NIS* and other thyroid-specific genes. When stimulated by lipopolysaccharide (LPS), NF-κB, especially the subunit p65, mediates an increase in expression of TSH with a subsequent induction of NIS and RAI uptake by interaction with the transcription factor PAX8 [38]. Interestingly, unlike LPS, stimulation with tumor-necrosis-factor-α (TNF-α) or phorbol-myristate-acetate (PMA) downregulates NIS expression following activation of NF-κB [39]. These differing effects on NIS transcription may be due to the activation and interaction of additional pathways that mediate the affinity of NF-κB transcription factors by the use of different gene promoters.

5.3.4 Targeted NIS gene therapy

Based on the role of NIS in RAI imaging and therapy in DTC, targeting NIS into thyroidal or extrathyroidal tumor environments followed by application of RAI or alternative radionuclides would provide a powerful new cytoreductive gene therapy strategy. The first report of a successful delivery of ^{125}I to a clonal variant FRLT thyroid cell line was demonstrated after rat NIS cDNA transfection and was described shortly after the cloning of NIS [40]. No significant reduction of tumor growth was observed after ^{131}I treatment in this study. Subsequent studies by Spitzweg *et al.* used the prostate specific antigen (PSA) promotor to selectively express NIS in the prostate cancer cells LNCaP. A significant tumor reduction was achieved after a single i.p. application of therapeutic ^{131}I in a subcutaneous NIS-transfected LNCaP model [41].

As a next important step in the application of NIS in non-NIS expressing tumors, a series of local gene delivery approaches were investigated for providing NIS gene transfer. The vector platforms most widely used in most preclinical and clinical studies are based on viruses. A study of local *NIS* gene delivery by intratumoral injections of adenovirus carrying the cytomegalovirus (CMV) promoter or tumor-specific carcinoembryonic antigen (CEA) promoter was conducted in a medullary thyroid cancer model [42]. The results demonstrated that *in vivo NIS* gene transfer using adenoviruses as delivery vehicles followed by RAI application resulted in a significant therapeutic effect in thyroid tumors. Intratumoral replication by a replicating virus was

found to help amplify the antitumor effect [43]. Later, a variety of studies focused on the potential use of specific gene promoters, such as the alpha-fetoprotein (AFP) or a prostate-specific (probasin) promoter to drive *NIS* transgene expression in different tumor models [44, 45]. A replication-selective adenovirus in which the *E1a* gene was driven by the AFP promoter with the NIS transgene inserted in the E3 region was intratumorally injected into HCC xenograft tumors, the combination of oncolytic virotherapy with radioiodine treatment resulted in a further reduction in tumor growth as compared to virotherapy alone [46].

However, the local gene delivery approaches used to date were generally not suitable for the treatment of metastatic disease. A crucial next step was to use systemic vector application to achieve tumor-selective NIS transgene expression in tumors and metastases. To this end a series of delivery vehicles that allow efficient systemic delivery of the NIS transgene have been investigated. A subset of the early studies used oncolytic virus-mediated NIS gene delivery in the treatment of various experimental tumors. Dingli *et al.* demonstrated in a preclinical study that systemic application of oncolytic measles virus (MV)-NIS enhanced the oncolytic potency of oncolytic measles viruses carrying the *NIS* gene in multiple myeloma tumor model and eliminated tumors resistant to the virus alone when combined with ^{131}I application [47]. Other studies had used various oncolytic virus-based approaches, including oncolytic vaccinia virus (VV) or oncolytic herpes simplex virus (HSV), engineered to express NIS in various tumor settings allowing monitoring of viral spread and replication, as well as stimulation of oncolytic potency by combination with NIS-mediated ^{131}I therapy, which showed enhanced therapeutic effect and prolonged survival of tumor-bearing mice [48-51]. These preclinical studies have provided a basis for a series of ongoing clinical trials using this biology: the systemic delivery of NIS encoding adenovirus (NCT00788307), measles virus (MV-NIS) (NCT02364713, NCT01503177, NCT02700230, NCT01846091, NCT02192775, NCT00408590, NCT00450814, NCT03456908) as well as vesicular stomatitis virus (NCT03120624, NCT03017820, NCT03647163) in various cancer types.

The use of viral vectors has demonstrated high transduction efficacy but safety issues such as an unwanted immune reaction, have limited the broader application of this approach. Further challenges include target selectivity and the manufacturing costs [52].

The use of synthetic non-viral vectors has emerged as a new research area. A series of non-viral approaches for systemic NIS gene delivery have been developed in the laboratory of Christine Spitzweg (LMU Munich) in co-operation with Prof. Dr. Ernst Wagner (LMU Munich). Dr. Kathrin Klutz conducted the first experiments of synthetic polymeric vectors for *NIS* gene therapy using oligoethylenimine (OEI)-grafted polypropylenimine dendrimers (G2-HD-OEI) complexed with *NIS* DNA (polyplexes) for the treatment of subcutaneous syngeneic neuroblastoma xenografts. The results showed a significant delay in tumor growth with dramatically improved survival [53]. The therapeutic effect was further validated in a subcutaneous HCC model [54]. In later studies, a novel linear polyethylenimine (LPEI), shielded by polyethylene glycol (PEG) attachment and coupled with the synthetic EGFR-specific peptide GE11 (LPEI-PEG-GE11) was used to optimize the tumor selectivity in an EGFR-overexpressing HCC model [55]. This application was further investigated in an anaplastic thyroid carcinoma (ATC) xenograft mouse model. Systemic injection of LPEI-PEG-GE11/NIS was used to reintroduce NIS into the ATC tumors followed by effective ^{131}I therapy showing reduced tumor growth and prolonged survival of animals [56].

As an additional promising gene delivery system, genetically engineered mesenchymal stem cells (MSCs) are currently being investigated based on their remarkable tumor homing capacity and straight forward isolation and transfection as discussed below.

5.4 Mesenchymal stem cells (MSCs)

5.4.1 Characteristics of MSCs

MSCs are known as non-hematopoietic progenitor cells that are found in many tissues including brain, liver, blood, and adipose tissue, and possess the ability to differentiate into multiple cell types, such as stromal cells, adipocytes, chondrocytes and osteocytes

[57]. They can be readily obtained from different tissues, such as bone marrow, adipose tissue. They are partially defined by a lack of major histocompatibility complex type II (MHCII) molecules and co-stimulatory ligands CD40, CD80, and CD86 expression, that help underly the ability of MSCs to be invisible to immune surveillance [58]. MSCs are known for their role in wound healing as they are recruited to sites of tissue injury and inflammation as 'first responders' [59]. They migrate to damaged tissue and organs to help tissue repair through differentiation and modulate the immune response [59, 60]. MSCs actively home to growing tumors which can be seen by the body as chronic wounds. This migration is thought to depend on the combined effects of chemokines, cytokines, and growth factors secreted by the tumor and the tumor microenvironment [58, 61, 62]. Based on these features MSCs are thought to be promising candidates to deliver anti-cancer agents or therapeutic genes to tumor sites.

5.4.2 Engineered MSCs as Gene Transfer Vehicles for targeted tumor therapy

Based on their inherent tropism for solid tumors, and their central role in tumor progression, genetically engineered MSCs have been used to deliver therapeutic agents into tumor microenvironments. One general approach has been to use engineered MSCs to constitutively secrete antitumor cytokines or factors such as β-interferon (IFN-β) [63], interleukin-2 (IL-2) [64], IL-12 [65], and also chemokine CX3CL1 [66] in the tumor environment that has led to decreased tumor growth and prolonged survival. MSCs were also modified to express tumor necrosis factor-α-related apoptosis-inducing ligand (TRAIL). Following recruitment of tumors, the engineered MSCs were shown to induce apoptosis of the tumor cells [67, 68].

An early strategy of MSC-based tumor therapy was to selectively target a suicide gene, such as herpes simplex virus thymidine kinase (HSV-TK) into pancreas, liver or breast tumors. When treated with the prodrug ganciclovir (GCV), it led to a toxic environment following phosphorylation by the enzymatic action of HSV-TK. The studies have shown

reduced tumor growth and incidence of metastasis [69-71]. A version of this approach has been used in phase I/II clinical trials at the University of Munich. The results showed that this MSC-based therapy was confirmed to be safe and tolerable in patients with advanced gastrointestinal adenocarcinoma [72].

MSCs have also been harnessed as delivery vehicles for oncolytic virus that selectively replicate and destroy cancer cells for the treatment of lung metastasis of breast carcinoma, ovarian carcinoma as well as glioma animal models. These studies showed that treatment resulted in decreased tumor burden and prolonged survival [73-75].

Another approach relied on the tumor migration of MSCs for directed cancer therapy by arming them with drug-loaded nanoparticles that release doxorubicin, docetaxel or paclitaxel into experimental models of lung cancer. The results obtained proved more efficient as compared with the conventional application of chemotherapeutic drugs [76-79].

In addition to the various approaches outlined above, one highly promising method is to systemically deliver the theranostic *NIS* gene in the context of MSCs as therapy vehicles.

5.4.3 MSC-based *NIS* transgene therapy

The application of the theranostic *NIS* gene represents an important step forward in the use of engineered MSC-based therapy vehicles. MSCs modified to express NIS can be monitored by radionuclide imaging. The functional NIS expression allows the tracking of MSC biodistribution before NIS-mediated radioiodine therapy. This allows an efficient demonstration of migration efficiency and provides a road map for therapeutic application of radioiodine.

The first study that made use of NIS-transfected MSCs was performed in the laboratory of Prof. Dr. Christine Spitzweg in collaboration with Prof. Dr. Peter Nelson, using the constitutively active CMV promoter to control NIS expression in the MSCs in a subcutaneous HCC mouse model [80]. The results demonstrated a high tumor selective radioiodine accumulation and efficient MSC-mediated NIS gene transfer to

the tumor environment. The subsequent ^{131}I therapy study showed a significant reduction in tumor growth as compared to control tumors with wild-type-MSCs.

A potentially important caveat in the use of MSCs as tumor therapy vehicles, is that a subset of the exogenously applied cells can migrate to non-tumor settings such as lymph nodes, skin, salivary glands and other normal tissue. This suggest that some off target effects may be seen in the course of therapy. To help limit the potential damage to normal tissues, our group has made use of gene promoters that efficiently respond to signals within the tumor environment to drive expression of the NIS transgene in engineered MSCs. The first study using NIS in this context was performed by Knoop *et al*. who made use of the inflammatory RANTES/CCL5 promoter to express NIS in MSCs. The approach was very successful in the treatment of a subcutaneous HCC model as well as in a colon cancer liver metastasis model. Both studies revealed robust MSC recruitment within the tumor stroma/metastasis and strong therapeutic effect after ^{131}I application [81, 82]. As hypoxia is one of the features of solid tumors, an additional approach was conducted where NIS gene expression in the MSCs was driven by a synthetic hypoxia responsive promoter in an orthotopic HCC xenograft mouse model. MSCs engineered with the NIS transgene driven by a synthetic hypoxia responsive promotor showed robust transgene induction under hypoxia both *in vitro* and *in vivo*. Administration of ^{131}I in mice treated with NIS engineered MSCs resulted in delayed tumor growth and prolonged survival [83]. Schug *et al*. investigated the effect of NIS-expressing MSCs where the NIS gene was driven by a synthetic TGF-β1-inducible SMAD-responsive promoter for the treatment of subcutaneous HCC xenografts [84]. The approach made use of the crucial role of TGF-β1 biology in HCC tumors. The results showed that the MSC SMAD-based NIS treatment induced significant radioiodine accumulation in the tumors resulting in a therapeutic effect of [131]I. Recently, Schmohl *et al*. successfully used MSCs engineered with a vascular endothelial growth factor (VEGF)-NIS reporter construct to target the angiogenic environment present in HCC xenografts [85]. Another study carried out by Dr. Mariella Tutter, tested the potential of using MSCs with a heat-inducible promoter, which allowed hyperthermia-

induced control of *NIS* gene expression and temperature-dependent accumulation of radioiodine in heat-treated tumors [86, 87].

In patients with recurrent ovarian cancer, an ongoing clinical study at the Mayo Clinic (Rochester, MN) is determining toxicity and effectiveness of intraperitoneal (i.p.) injection of genetically modified MSCs delivering measles virus expressing NIS as a reporter gene (NCT02068794).

6. Aims of this thesis

Our previous work in the field of NIS-based gene therapy has demonstrated the potential of genetically engineered MSCs as tumor-selective *NIS* transgene delivery vehicles. NIS allows detailed non-invasive *in vivo* tracking of MSC by ^{123}I-scintigraphy or [124]I-PET imaging, as well as highly effective therapeutic application of radionuclides (^{131}I, [188]Re). The goal of this thesis was to evaluate the effectiveness and tumor-selectivity of NIS mediated NIS gene therapy in RAI-refractory thyroid cancer using MSCs genetically engineered to drive the NIS transgene by TGF-β-based signaling. The following questions were addressed.

1. TGF-β1 plays an important role in the development of RAI-refractory thyroid cancer. We sought to characterize TGF-β expression in a series of thyroid cancer cell lines and determine if it is sufficient to induce functional NIS expression in MSCs using a synthetic TGF-β1-inducible/SMAD-responsive promoter to drive NIS transgene expression (SMAD-NIS-MSCs).

2. To further characterize the importance of TGF-β secretion by thyroid cancers in tumor-directed MSC migration using a 3D chemotaxis assay.

3. To characterize *in vivo* the actions of SMAD-NIS-MSCs in thyroid cancer xenografts through ^{123}I-scintigraphy, and determine the level of therapy effect achieved following application of [131]I.

7. Materials and methods

7.1 Cell lines

The human papillary thyroid cancer cell lines BCPAP, MDA-T41, MDA-T120, MDT-T32 and anaplastic thyroid cancer cell lines 8305C, 8505C, SW1736, BHT101 and HTh74 were cultured in RPMI1640 culture medium (Sigma Aldrich, St. Louis, Missouri, USA) supplemented with 10% (v/v) Fetal Bovine Serum (FBS) (Sigma-Aldrich) and 100 U/ml penicillin and 100 µg/ml streptomycin (P/S; Sigma-Aldrich). The human papillary thyroid cancer cell line K1 was grown in DMEM: Ham's F12: MCDB 105 (2:1:1) supplemented with 10% (v/v) FBS, 2mM Glutamine and P/S. The human anaplastic thyroid cancer cell lines HTC-C3 was cultured in DMEM (high glucose) supplemented with 20% FBS and P/S. The human follicular thyroid cancer cell lines FTC-133 and ML-1 were cultured in DMEM/Ham's F12 supplemented with FBS and P/S. All cells were maintained at 37 ℃, 5% CO_2 and 95% relative humidity. Cell culture medium was replaced every 2-3 days and the cells were passaged at 70%-90% confluency.

7.2 SMAD-NIS-MSCs

Human bone marrow-derived mesenchymal stem cells were cultured in RPMI1640 supplemented with 10% FBS and P/S. Wild type MSCs (WT-MSCs) had been stably transfected with pcDNA6-2ITRNEO-SMAD-NIS expression vector as previously described [84]. The stably transfected SMAD-NIS-MSCs were maintained in RPMI1640 supplemented with 10% FBS, P/S and 0.5 mg/ml G418.

7.3 Tumor cell line conditioned medium (CM)

$1×10^6$ tumor cells were seeded on 100 mm cell culture dishes for 24 h and starved overnight. Medium was exchanged by fresh medium without FBS. Conditioned growth media from the tumor cell line was collected after 48 h, centrifuged and stored at -80 ℃.

7.4 Quantitative real-time PCR

Total RNA from tumor cells was isolated with TRIzol Reagent according to the manufacturer's instructions. Reverse transcription was performed using SuperScript III reverse transcriptase. Quantitative real-time PCR was performed using the SYBR green PCR master mix in a Mastercycler ep gradient S PCR cycler. The following primers were used: () *ACTB* (β-actin): forward primer (5'-AAGAGCTATGAGCTGCCTGA-3'), reverse primer (5'-TACGGATGTCAACGTCACAC-3') ; *18S rRNA* (R18s) : forward primer (5'-CGCAGCTAGGAATAATGGAA-3'), reverse primer (5'-TCTGATCGTCTTCGAACCTC-3'); *TGF-β1*: forward primer, (5′-CAGCACGTGGAGCTGTACC-3′), reverse primer (5′-AAGATAACCACTCTGGCGAGTC-3′); *TGF-β2*: forward primer (5'-GTGCTTTGGATGCGGCCTA-3') , reverse primer (5'-GGCATGCTCCAGCACAGAA-3'); *TGF-β3*: forward primer (5'-CAAAGGCGTGGACAATGAGG-3'), reverse primer (5'-ACTTCCAGCCCAGATCCTGT-3'); *NIS*: forward primer (5'-TGCTAAGTGGCTTCTGGGTTGT-3'), reverse primer (5'-ATGCTGGTGGATGCTGTGCTGA-3'). Relative expression level of TGF-β1, TGF-β2, TGF-β3, NIS were calculated from ΔΔCt values normalized to internal β-actin and 18S rRNA.

7.5 ELISA

An ELISA assay for TGF-β1 was performed on the tumor conditioned medium using the human TGF-β1 DuoSet ELISA kit (R&D Systems, Abington, UK) following the manufacturer's instructions.

7.6 CM stimulation of the SMAD-NIS-MSCs and ^{125}I uptake assay

0.3×10^6 SMAD-NIS-MSCs were seeded on 6-well plates. After starvation with serum-free medium overnight, medium was exchanged by 80% (v/v) normal culture medium and 20% (v/v) tumor conditioned medium for 24 h. NIS mediated ^{125}I uptake of the MSCs was measured according to a previously described iodide uptake assay [88].

For control experiments, to validate the SMAD-based promoter inducibility, the TGF-β1 receptor inhibitor EW-7197 (vactosertib; Selleckchem) (0.5 µmol/L) was used. The NIS-specific inhibitor $KClO_4$ (100 mM; Merck Millipore, Burlington, Massachusetts, USA) was added to verify NIS specificity of uptake. All the results were normalized to cell viability and shown as cpm/A620.

7.7 Cell viability assay

The commercially available MTT (3-(4,5-dimethylthiazol-2-yl)-2,5-diphenyltetrazolium bromide) assay (Sigma Aldrich) was performed according to the manufacturer's recommendations. The absorbance was measured on a Sunrise microplate absorbance reader (Tecan, Mannedorf, Switzerland) at a wavelength of 620 nm using the software Magellan (Tecan).

7.8 Co-culture of SMAD-NIS-MSCs and tumor cell lines

TGF-β-induced functional NIS expression in SMAD-NIS-MSCs was also measured by ^{125}I uptake assay in SMAD-NIS-MSCs that are co-cultured with the thyroid cancer cells at different ratios. 1.5×10^5 of tumor cells and 1.5×10^5 MSCs were defined as 1:1. As a control, to confirm that the activation of the SMAD-responsive promoter in SMAD-NIS-MSC was TGF-β induced, co-incubations with the TGF-β1 receptor inhibitor EW-7197 (0.5 µmol/L) was performed.

7.9 3D migration assay

Migration assay was performed using the µ-slide Chemotaxis 3D system from ibidi (Martinsried, Germany). SMAD-NIS-MSCs were seeded in Collagen I (0.5×10^6) and exposed to a gradient between serum-free medium and BCPAP or K1 conditioned medium with or without the TGF-β1 receptor inhibitor EW-7197. Monitoring of the migration assay was done as previously described [89]. 20 randomly selected cells were manually tracked and analyzed with Chemotaxis and Migration Tool software (ibidi). The forward migration index (FMI) and the center-of-mass (CoM) were

calculated for all tracked cells to quantify the migratory behavior of the SMAD-NIS-MSCs.

7.10 Spheroid formation

1 g Poly-HEMA (Poly 2-hydroxyethyl methacrylate) (Sigma Aldrich) were dissolved in 50 ml 95% ethanol at 60 ℃ to get a 2% solution. 100 mm dishes were covered by 2 ml poly-HEMA solution and left without lids in the tissue-culture hood to dry completely overnight. This step was repeated once to create a smooth layer. All the dishes were sterilized by exposing to ultraviolet light for over 30 min. 1×10^6 tumor cells were cultivated in the poly-HEMA coated dishes in an incubator (37 ℃, 5% CO_2) for seven days to form proper-size spheroids. Supernatants of the spheroids (spheroids CM) were collected 48 h after changing the serum-free medium, centrifuged and stored at -80 ℃.

7.11 K1 and BCPAP xenograft mouse models

Female 5-week-old CD1 nu/nu mice were bought from Charles River (Sulzfeld, Germany) and maintained under specific pathogen-free conditions with *ad libitum* access to water and standard nude mouse diet. The experiments were authorized by the regional governmental commission for animals (Regierung von Oberbayern, Munich, Germany). To establish xenograft tumors, 2×10^6 K1 cells or 15×10^6 BCPAP cells in 50 µl PBS and 50 µl Matrigel were injected subcutaneously into the right flank region of the mice. Tumors were regularly measured using a caliper and calculated using the equation: length × width × height × 0.52. Mice were sacrificed when the tumor reached a volume of 1500 mm^3.

7.12 ^{123}I-scintigraphy imaging

When subcutaneous tumors (K1 and BCPAP) reached a volume of approx. 500 mm^3, drinking water was supplemented with 5 mg/ml L-thyroxine (L-T4; Sigma-Aldrich) and the animals were given iodine deficient food (ssniff Spezialdiaten GmbH, Soest, Germany) for ten days prior to radioiodine application to suppress thyroidal iodide

uptake. 5×10^5 SMAD-NIS-MSCs or WT-MSCs in 500 µl PBS were applied three times every second day via the tail vein. 72 h after the last MSCs injection, 18.5 MBq (0.5 mCi) of ^{123}I were intraperitoneally injected into the mice. As a control group, each mouse received 2 mg of the competitive NIS inhibitor sodium perchlorate (Sigma-Aldrich) 30 minutes before ^{123}I injection. Radioiodine biodistribution was measured using a gamma camera (e.cam; Siemens, Erlangen, Germany) equipped with a low-energy, high-resolution collimator. To evaluate the tumoral radioiodine uptake, the regions of interests (ROIs) were calculated by measuring the percentage of the total injected radioiodine dose per tumor (% ID/tumor) using the HERMES GOLD (Hermes Medical Solutions, Stockholm, Sweden) software.

7.13 Immunohistochemical NIS and TGF-β1 protein staining

Xenograft tumors were dissected from all the mice after imaging study and embedded in paraffin. Immunohistochemical NIS staining of paraffin-embedded tumor sections were performed as previously described [42]. Briefly the sections were incubated with a primary mouse monoclonal NIS-specific antibody (Merck Millipore; dilution 1:500) for 60 min followed by a biotin-SP-conjugated goat anti-mouse IgG antibody (Jackson Immunoresearch; dilution 1:200) for 20 min followed by peroxidase-conjugated streptavidin (Jackson Immunoresearch; dilution 1:300) for an additional 20 min. Tissue sections were scanned using the Pannoramic MIDI digital slide scanner and pictures were taken with Caseviewer software (3DHISTECH Ltd., Budapest, Hungary). Immunohistochemical staining of TGF-β1 protein was conducted on tumor sections with an antibody ab92486 (Abcam, Cambridge, UK) as described previously [84].

7.14 ^{131}I therapy study

Therapy trials were started when the tumors (K1 and BCPAP) reached an average size of 50 mm^3. Ten days before the radioiodine injection, all mice received drinking water supplemented with 5 mg/ml L-T4 (Sigma-Aldrich) and iodine deficient food to minimize the iodine uptake by the thyroid gland thus enhancing tumoral iodine accumulation. For the therapy group, SMAD-NIS-MSCs (5×10^5 cells in 500 µl PBS) were injected

intravenously (i.v.) on every second day three times followed by a 55.5 MBq ^{131}I application 48 hours after the last SMAD-NIS-MSC injection (K1: SMAD-NIS-MSCs + [131]I; n=7) (BCPAP: SMAD-NIS-MSCs + [131]I; n=9). 24h after the radioiodine application this cycle was repeated. One additional MSCs injection followed by a third ^{131}I application was done for a complete therapy trial. To clarify the therapeutic effect of SMAD-NIS-MSCs, same amount of WT-MSCs were applied to the mice instead of SMAD-NIS-MSCs (K1: WT-MSCs + [131]I; n=5) (BCPAP: WT-MSCs + [131]I; n=8). As further controls, a subset of mice received saline (NaCl) instead of [131]I (K1: SMAD-NIS-MSCs + NaCl; n=6) (BCPAP: SMAD-NIS-MSCs + NaCl; n=10) and another group was injected with NaCl only (K1: NaCl + NaCl; n=7) (BCPAP: NaCl + NaCl; n=7). Tumor volume was evaluated regularly as described and mice were sacrificed when a tumor volume of 1500 mm^3 was exceeded or when tumors started to ulcerate.

7.15 *Ex vivo* immunofluorescence assay

Frozen sections of dissected tumors from the ^{131}I therapy study were immunofluorescence stained for the analysis of cellular proliferation (Ki67) and blood vessel density (CD31) as previously described [90]. All sections were incubated with a rabbit polyclonal antibody against human Ki67 (Abcam, Cambridge, UK; dilution 1:100) and a rat monoclonal antibody against mouse CD31 (BD Pharmingen, Heidelberg, Germany; dilution 1:200) for 2 h at room temperature followed by incubation with an anti-rabbit Alexa488-conjugated antibody (Jackson ImmunoResearch) for Ki67 staining and an anti-rat Cy3-conjugated antibody (Jackson ImmunoResearch) for CD31 staining. Nuclei were counterstained with Hoechst bisbenzimide (5 mg/ml). Stained sections were scanned with the Pannoramic MIDI digital slide scanner with identical exposure time. Quantification of the percentage of positive cell for Ki67 and positive area for CD31 was performed by evaluation of 5 high-power fields per tumor using ImageJ software (NIH Bethesda, MD).

7.16 Statistical analysis

All *in vitro* experiments were repeated at least in triplicate. Results were presented as mean ± standard error of the mean (SEM), mean fold change ± SEM or percentage for survival plots and analyzed using SPSS 26 (IBM, USA). Statistical significance was tested by independent samples t-Test, and one-way ANOVA (data with homogeneous variances) or Welch test (data with unequal variances) for comparison of more than two groups. For the post-hoc test, Tukey-HSD test was used for data with homogeneous variances and Tamhane's T2 test for data with unequal variances. Log-rank test was used for the survival plots. *p* values <0.05 were considered significant (*p<0.05; **p<0.01; ***p<0.001).

8. Results

A central goal of the present thesis was to evaluate the use of MSCs engineered to selectively express NIS as a potential treatment of RAI-refractory thyroid cancer. To this end, we sought to selectivity trigger MSC-NIS expression within the tumor environment through use of a synthetic TGF-β-responsive gene promoter (SMAD-responsive). The enhanced presence of TGF-β within the tumor environment should allow selective activation of NIS by the MSCs following tumor recruitment. As a first step, a series of thyroid tumor lines were evaluated for expression of TGF-β.

## 8.1 *In vitro* TGF-β mRNA and proteins levels in different tumor cell lines

TGF-β expression has been described to be increased in some thyroid tumors. To characterize TGF-β expression in RAI-refractory thyroid cancer cell lines, 13 NIS-negative thyroid cancer cell lines representing PTC, FTC and ATC were evaluated for their mRNA expression of TGF-β1, TGF-β2 and TGF-β3 (Fig 1). All cell lines were verified to have relatively high levels of TGF-β1 expression. BCPAP showed the highest TGF-β1 level, while K1, 8505C and BHT101 showing lowest TGF-β1 expression (Fig 1A). For TGF-β2, only MDA-T41, MDA-T120, BHT101, FTC-133, SW1736, MDA-T32 and BCPAP showed expression (Fig 1B). TGF-β3 was largely absent in all the thyroid cancer cell lines tested (Fig 1C).
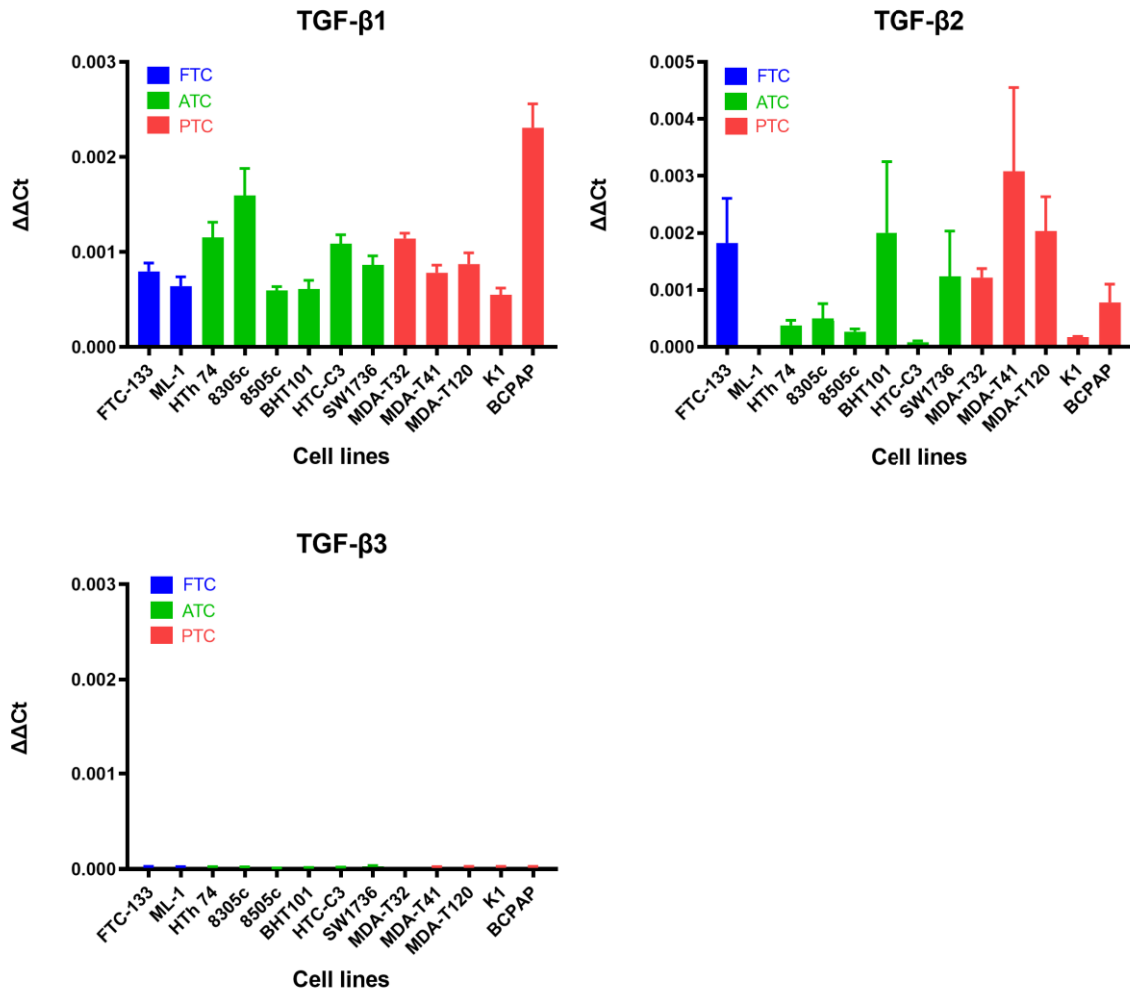
Figure 1. TGF-β expression in thyroid cancer cell lines. *qRT-PCR analysis of TGF-β1, 2, 3 mRNA extracted from human FTC cell lines FTC-133 and ML-1, ATC cell lines HTh74, 8305C, 8505C, BHT101, HTC-C3 and SW-1736, and PTC cell lines MDA-T32, MDA-T41, MDA-T120, K1 and BCPAP **(A-C)**. Data are represented as mean values ± SEM (n=3).*

To further evaluate TGF-β1 expression at the protein level, ELISA was performed on the conditioned medium from each cell line (Fig 2). The ELISA used allowed detection of active TGF-β1, and by treating the conditioned media with 1 N HCl followed by 1.2 N NaOH it was possible to discriminate between levels of latent and active protein present in the growth medium. All the cell lines showed TGF-β1 secretion into the CM. K1 showed the lowest level of latent and activated TGF-β1 levels, whereas the highest levels were seen in FTC-133, HTh74, MDA-T32, MDA-T120 and BCPAP.
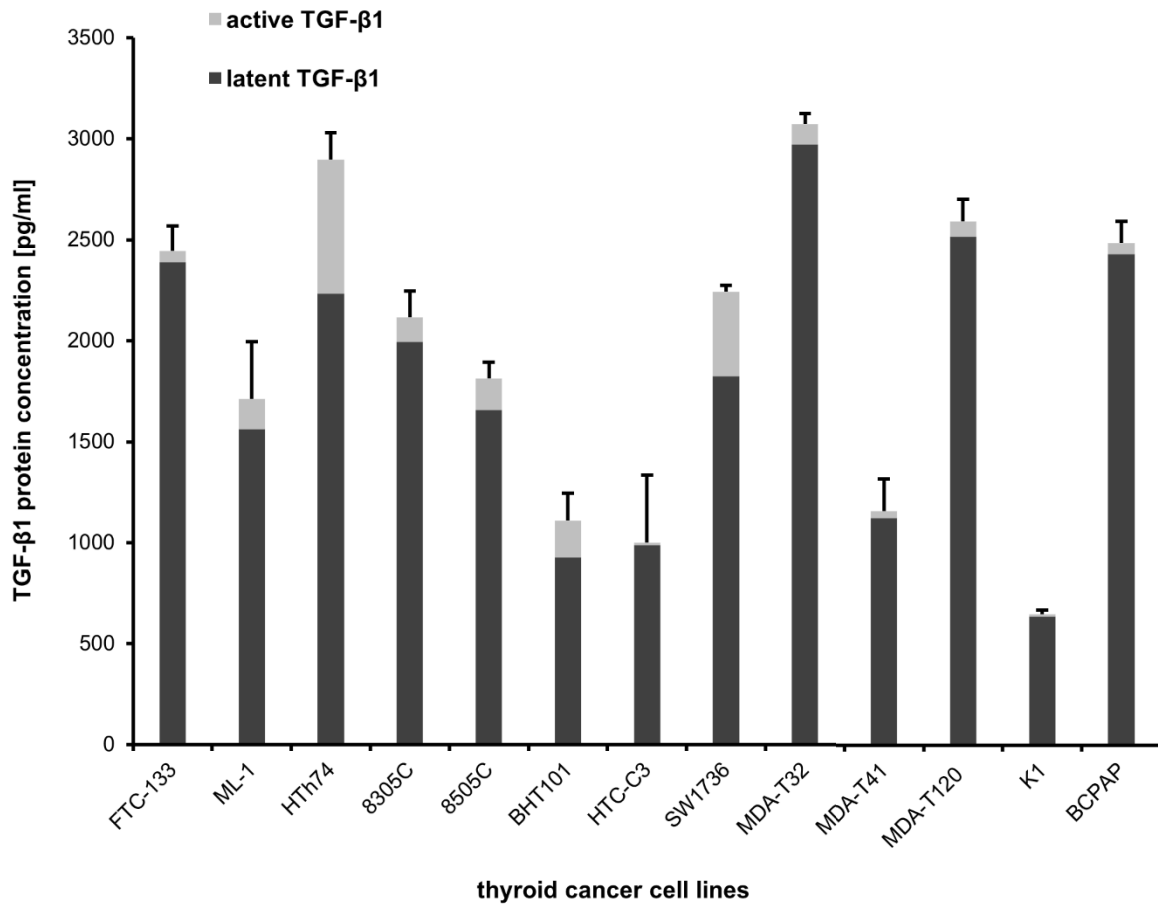
Figure 2. TGF-β1 protein expression analysis of different thyroid cancer cells in vitro. *Active and latent TGF-β1 protein levels in conditioned medium derived from thyroid cancer cell lines were assessed by ELISA. Latent TGF-β1 was activated to be detected by treating the conditioned medium with the activation reagents (1 N HCl followed by 1.2 N NaOH). Data are represented as mean values ± SEM (n=3).*

8.2 Stimulation of NIS-mediated radioiodine accumulation in SMAD-NIS-MSCs by tumor conditioned medium

A

B
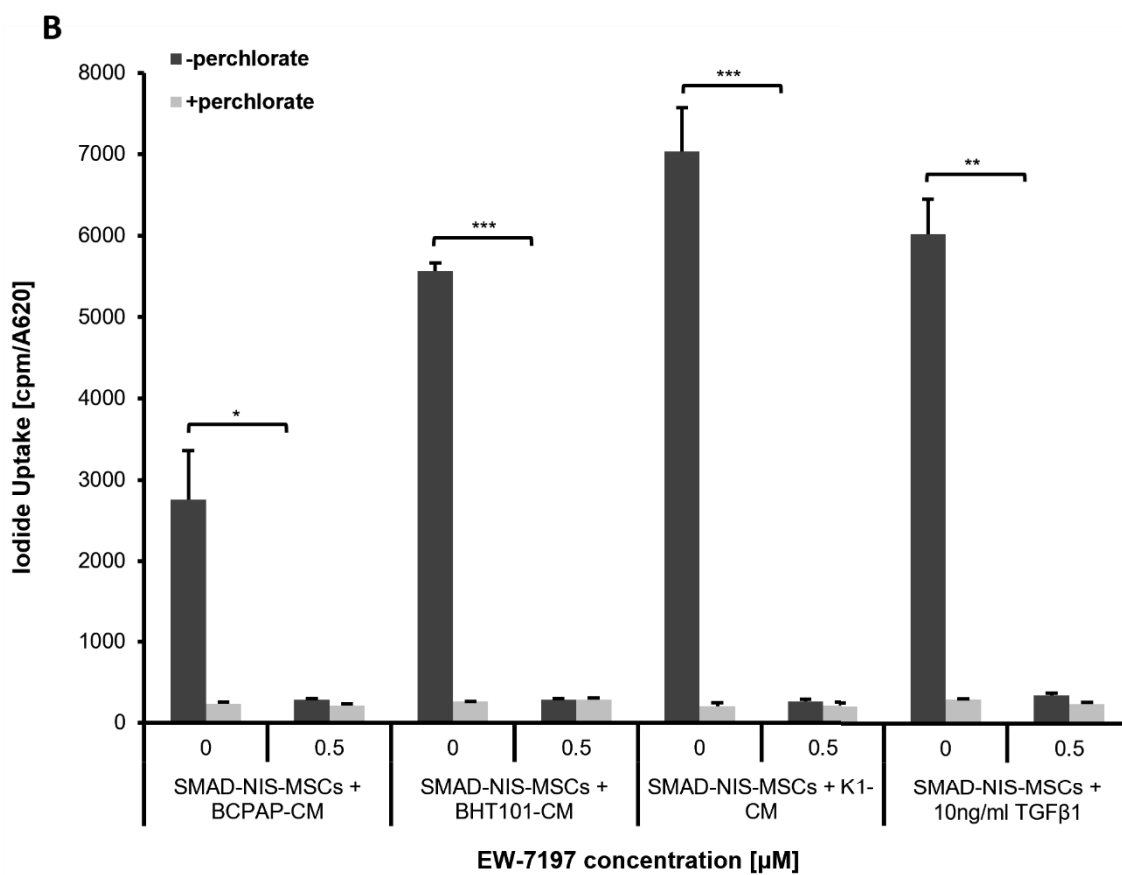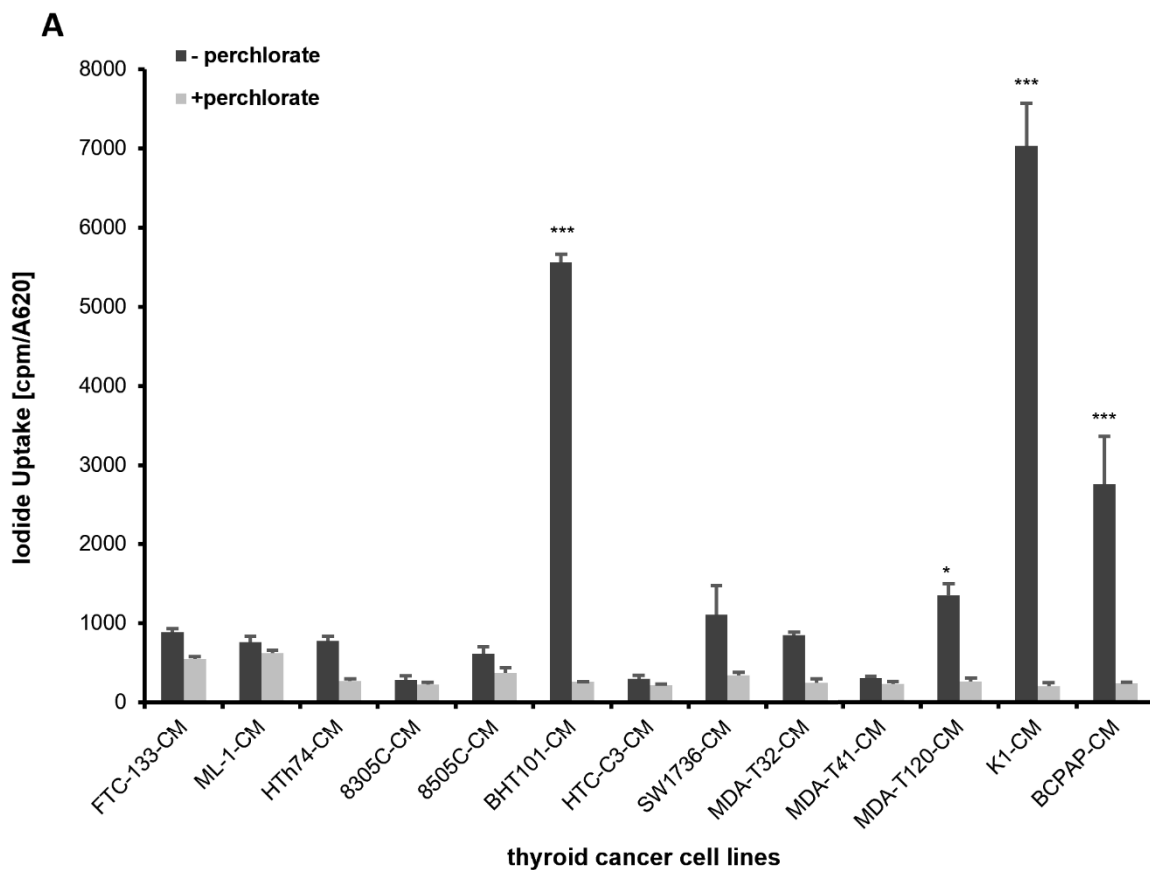
Figure 3. SMAD-NIS-MSCs stably expressing NIS stimulated by tumor conditioned medium. ^{125}I uptake studies demonstrated significant higher NIS-specific, perchlorate-sensitive iodide uptake in SMAD-NIS-MSCs stimulated with BHT101-CM, MDA-T120-CM, K1-CM and BCPAP-CM as compared with unstimulated cells **(A)**. Data are represented as means of three independent experiments ± SEM (n=3; one-way ANOVA: *p<0.05; **p<0.01, ***p<0.001). Treatment with the selective TGF-β1 receptor ALK4/ALK5 inhibitor EW-7197 resulted in complete inhibition of radioiodine uptake in conditioned medium treated SMAD-NIS-MSCs demonstrating the selective stimulation of the SMAD-responsive promoter in SMAD-NIS-MSCs through TGFβ-1 **(B)**. Data are represented as means of three independent experiments ± SEM (n=3; independent samples t-Test: *p<0.05; **p<0.01; ***p<0.001)

Since the tumor cell lines showed variation in the amount of TGF-β1 secretion, the ability of the tumor CM to activate NIS expression in the engineered MSCs was evaluated. Conditioned media diluted 1:4 with normal medium was used to stimulate SMAD-NIS-MSCs. The SMAD-NIS-MSCs cultured with normal medium alone did not show iodide accumulation in radioiodine uptake assays. The stimulation of MSCs with conditioned medium from BHT101, MDA-T120, K1 and BCPAP cells resulted in a significant increase of iodide accumulation, while a slight increase was seen in the other tumor CM (Fig 3A).

Interestingly the highest iodide uptake (22.9-fold increase) was found when K1-CM was used which had the lowest level of TGF-β1 secretion. To confirm the NIS-specificity, the NIS-specific inhibitor perchlorate was used in all the groups, which showed full blockage of the iodide uptake (Fig 3A).

To further verify the specificity of NIS expression induced by TGF-β1 in SMAD-NIS-MSCs, SMAD-NIS-MSCs stimulated by BHT101-CM, K1-CM, BCPAP-CM or 10ng/ml TGF-β1 were additionally treated with the selective TGF-β1 receptor ALK4/ALK5 inhibitor EW-7197 (0.5 μmol/L). SMAD-NIS-MSCs showed complete inhibition of radioiodine uptake upon treatment with EW-7197 in all groups (Fig 3B).

8.3 Stimulation of functional NIS expression in SMAD-NIS-MSCs by co-culture with thyroid cancer cell lines

In parallel, to further validate NIS expression in SMAD-NIS-MSCs introduced by signals derived from tumor cells, three tumor cell lines (BCPAP, BHT101 and K1) were directly co-cultured with SMAD-NIS-MSCs at different tumor cell to MSC ratios. No radioiodine uptake activities were seen in tumor cell lines alone demonstrating the lack of functional NIS expression in these cell lines. SMAD-NIS-MSCs co-cultured with BCPAP showed the highest level of radioiodine uptake as compared to co-culture with the other two cell lines. The strongest signal from the BCPAP line was seen at a ratio of 1 MSC:1 BCPAP cell. BHT101 also successfully induced NIS expression in SMAD-NIS-MSCs with the best results seen at a ratio of 2 MSC:1 BHT101. K1 showed a slight stimulation of NIS expression in SMAD-NIS-MSCs at the ratio 1 MSC:1 K1. Treatment with perchlorate confirmed the NIS specificity in the radioiodine uptake assays, and use of the TGF-β1 receptor inhibitor EW7197 demonstrated TGF-β1 specificity of NIS induction (Fig 4).
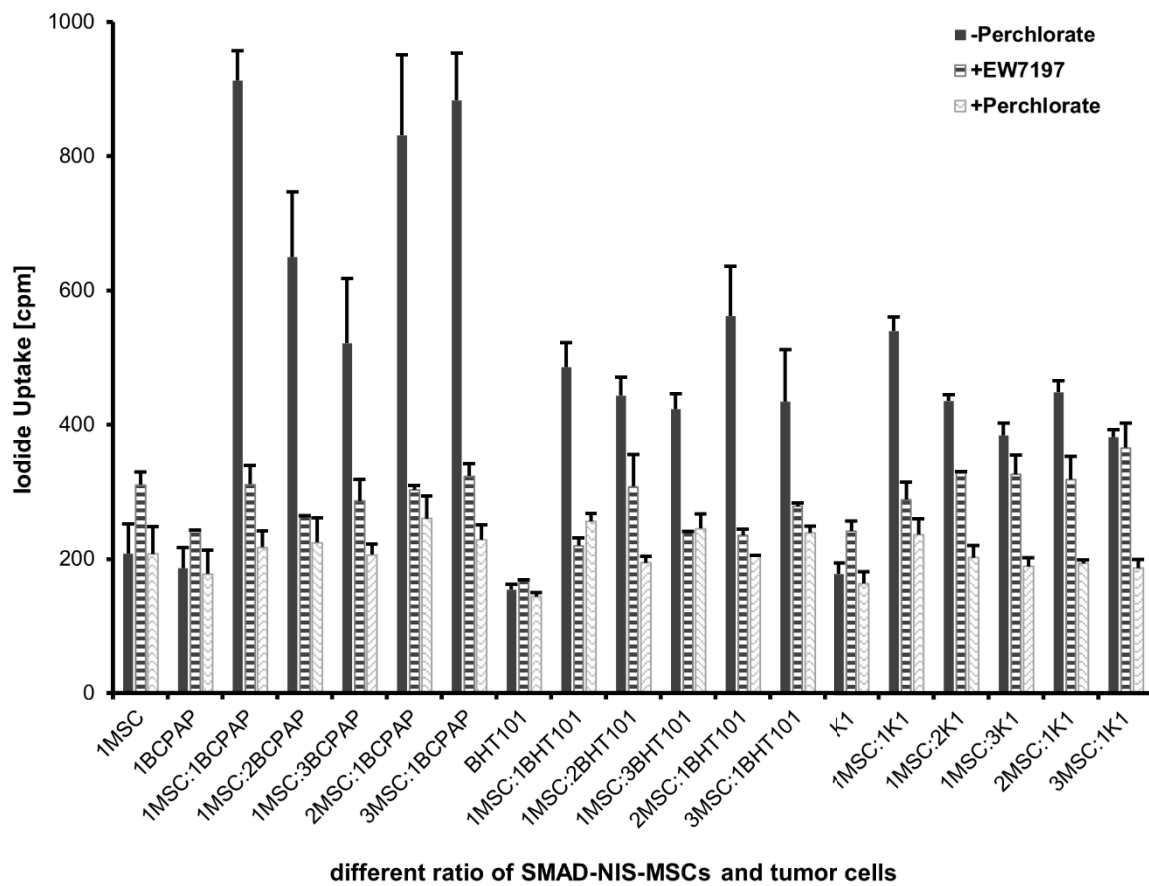
Figure 4. SMAD-NIS-MSCs co-cultured with thyroid cancer cell lines. *No radioiodine uptake was seen in MSCs or tumor cells alone. MSCs co-cultured with BCPAP, BHT101 and K1 cells showed increased iodide uptake with the highest seen at cell ratios of 1:1 (MSC: BCPAP), 2:1 (MSC: BHT101), 1:1 (MSC: K1) respectively. Treatment with perchlorate or the TGF-β1 receptor inhibitor EW-7197 resulted in inhibition of radioiodine uptake demonstrating the NIS-specificity of iodide accumulation and TGF-β specificity of induction of functional NIS expression, respectively. Data are represented as means of three independent experiments ± SEM (n=3).*

8.4 MSCs showed directed migration towards tumor derived signals

Based on the results as presented above, the tumor cell lines tested secreted sufficient TGF-β1 to activate the SMAD responsive promotor in the SMAD-NIS-MSCs. To establish the potential effect of TGF-β1 on the directed migration of MSCs, a 3D chemotaxis assay was applied. SMAD-NIS-MSCs were subjected to untreated normal medium in both chambers to demonstrate a lack of chemotaxis and to control for chemokinesis (Fig 5A). MSCs showed non-directed chemotaxis towards recombinant TGF-β1 (Fig 5B) but with an increase in mean center of mass (yCoM; red dots) (Fig 5G) and mean forward migration index (yFMI) (Fig 5H). Cells under the influence of a gradient between untreated medium and tumor CM, showed directed chemotaxis (Rayleigh values $p<0.05$) (Fig 5C, E) and a significant increase in yCoM and yFMI towards the BCPAP-CM and K1-CM as compared to untreated medium (Fig 5G, H). SMAD-NIS-MSCs showed only random migration when subjected to untreated medium and tumor CM in addition with EW-7197 (Fig 5D, F).
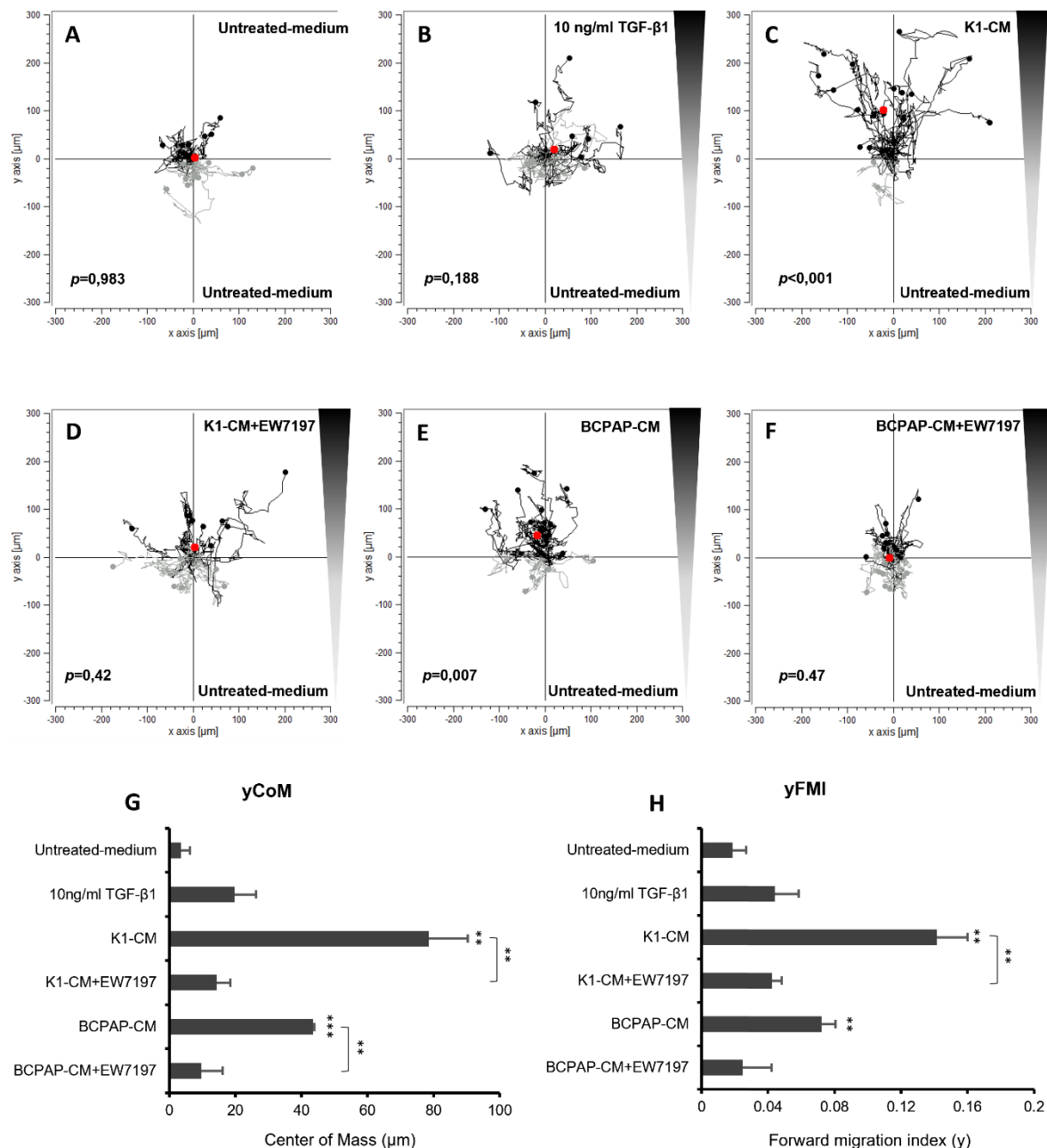
Figure 5. Chemotactic behavior of SMAD-NIS-MSCs confirmed by chemotaxis assay. *SMAD-NIS-MSCs subjected to untreated medium in both chambers showed no directed chemotaxis **(A)**. MSCs showed non-directed chemotaxis towards TGFB1 **(B)** but with an increase in mean center of mass (yCoM; red dots) **(G)** and mean forward migration index (yFMI) **(H)**. Cells under the influence of a gradient between untreated medium and tumor CM, showed directed chemotaxis **(C, E;** Rayleigh values p<0.05**)** and a significant increase in yCoM and yFMI towards the BCPAP-CM and K1-CM compared to untreated medium **(G, H;** independent samples t-Test: ****p<0.01, ***p<0.001)**. SMAD-NIS-MSCs only showed random migration when subjected to*

*untreated medium and tumor CM in addition with EW-7197 **(D, F)**. Data are represented as mean values± SEM from three independent experiments.*

8.5 Tumor cell spheroids
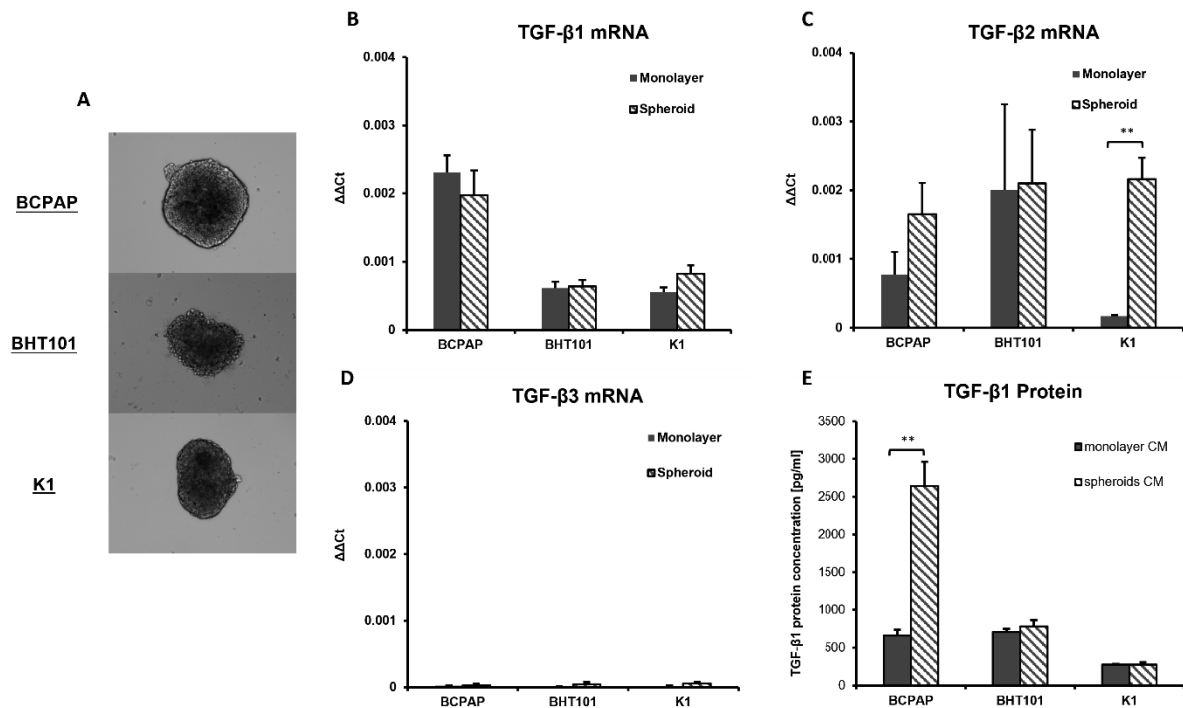
***Figure 6. TGF-β mRNA and protein levels in tumor spheroids.** BCPAP, BHT101 and K1 spheroids were generated by culturing on Poly-HEMA coated plates **(A)**. qRT-PCR analysis of mRNA extracted from monolayer cells and spheroids using primers for TGF-β1 **(B)**, TGF-β2 **(C)** and TGF-β3 **(D)**. TGF-β1 protein levels in conditioned medium were assessed by ELISA **(E)**. Results were normalized by cell numbers. Data are represented as means of three independent experiments ± SEM (n=3; independent samples t-Test: **p<0.01)*

To better mimic the *in vivo* tumor microenvironments of the tumors, 3-dimensional thyroid cancer cell spheroids were established. An optional size of BCPAP, BHT101 and K1 spheroids were generated by culturing the cell line on Poly-HEMA coated

plates for 7 days (Fig 6A). TGF-β1, TGF-β2 and TGF-β3 mRNA levels were evaluated by qRT-PCR. The BCPAP spheroids showed slightly lower TGF-β1 expression as compared to the monolayer cells, but a 2-fold increase in the level of TGF-β2 mRNA (Fig 6B, C). For the K1 spheroids, both TGF-β1, TGF-β2 were increased as compared to the monolayers (Fig 6B, C). No differences were seen in the BHT101 spheroids as compared to monoculture (Fig 6B, C). All three spheroids showed very low TGF-β3 levels which was also seen in monolayer cells (Fig 6D). TGF-β1 protein secretion in CM was investigated by ELISA and normalized to cell numbers. A significant increase in TGF-β1 protein was seen in BCPAP spheroids as compared to monolayer while no differences were seen between BHT101 or K1 spheroids and monolayer cells (Fig 6E).

8.6 *In vivo* ^{123}I-scintigraphy imaging after MSC-mediated *NIS* gene transfer in thyroid cancer xenograft mouse models

Based on their expression of TGF-β, the BCPAP and K1 cell lines were selected to establish subcutaneous mouse models. 2×10^6 K1 cells or 15×10^6 BCPAP cells in 50 μl PBS and 50 μl Matrigel were injected into the right flank region of the mice. After 5-7 weeks when subcutaneous tumor reached an approximate volume of 500-700 mm^3, 5×10^5 SMAD-NIS-MSCs in 500 μl PBS were injected into the tumor-bearing nude mice via the tail vein three times at 48 h intervals. 72 h after the last MSCs application, 18.5 MBq ^{123}I were administered intraperitoneally and the radioiodine biodistribution was analyzed using ^{123}I-scintigraphy. The images revealed a maximum tumoral iodide accumulation one hour post ^{123}I injection with approximately 6.72±0.67% of the injected dose per tumor in K1 subcutaneous tumors after SMAD-NIS-MSC application (Fig 7A, G), whereas BCPAP subcutaneous tumors accumulated 8.40±0.42% (Fig 7D, G). Physiological NIS-mediated radioiodine uptake was seen in the thyroid, salivary glands and stomach. Radioiodine accumulation seem in the urine bladder was due to renal elimination of [123]I.

To confirm that the tumoral ^{123}I accumulation was NIS-mediated, a group of control mice were injected with WT-MSCs instead of SMAD-NIS-MSCs. These mice showed no radioiodine uptake in tumors (Fig 7B, E). In an additional control group of mice injected with SMAD-NIS-MSCs, pretreatment of perchlorate 30 min prior to ^{123}I administration inhibited the tumoral accumulation of radioiodine in both models (Fig 7C, F).
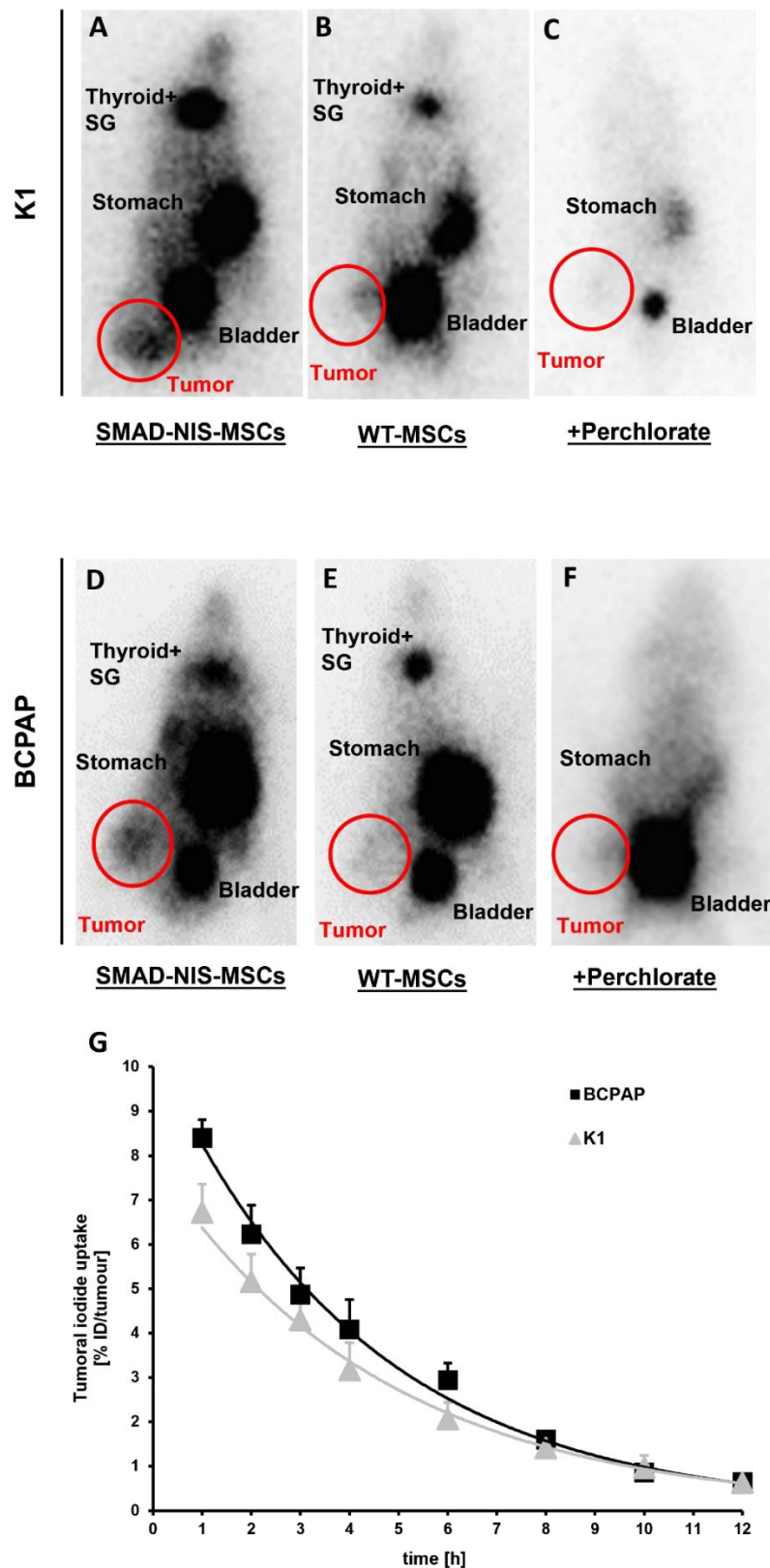
Figure 7. In vivo ^{123}I-scintigraghy of NIS-mediated iodide uptake in K1 and BCPAP xenografts. *Three intravenous injections of SMAD-NIS-MSCs in mice harboring subcutaneous K1 (A) tumors and BCPAP (D) tumors resulted in tumor-specific radioiodine uptake that was perchlorate sensitive (C, F). Injection of WT-MSCs*

*instead of SMAD-NIS-MSCs resulted in no tumor-specific radioiodine uptake in both models **(B, E)**. SG: salivary gland. Radioiodine retention time in tumors was determined by serial scanning over 12h **(G)**. Data are represented as means values ± SEM.*

8.7 *Ex vivo* NIS and TGF-β1 expression analysis in dissected tumors

After establishing the functional distribution of NIS transgene expression by ^{123}I-scintigraphy, paraffin-embedded tumor tissue sections were stained immunohistochemically to more selectively evaluate the biodistribution of SMAD-NIS-MSCs within the experimental tumors. The staining revealed NIS-specific immunoreactivity (red) in both BCPAP xenograft tumor (Fig 8D) and K1 xenograft tumor (Fig 8A) throughout the tumor stroma after application of SMAD-NIS-MSCs, while no NIS-specific immunostaining was observed after WT-MSCs injection (Fig 8B, E). TGF-β1 staining in subcutaneous BCPAP and K1 tumors indicated a strong TGF-β1 expression within the tumor stroma (Fig 8C, F).
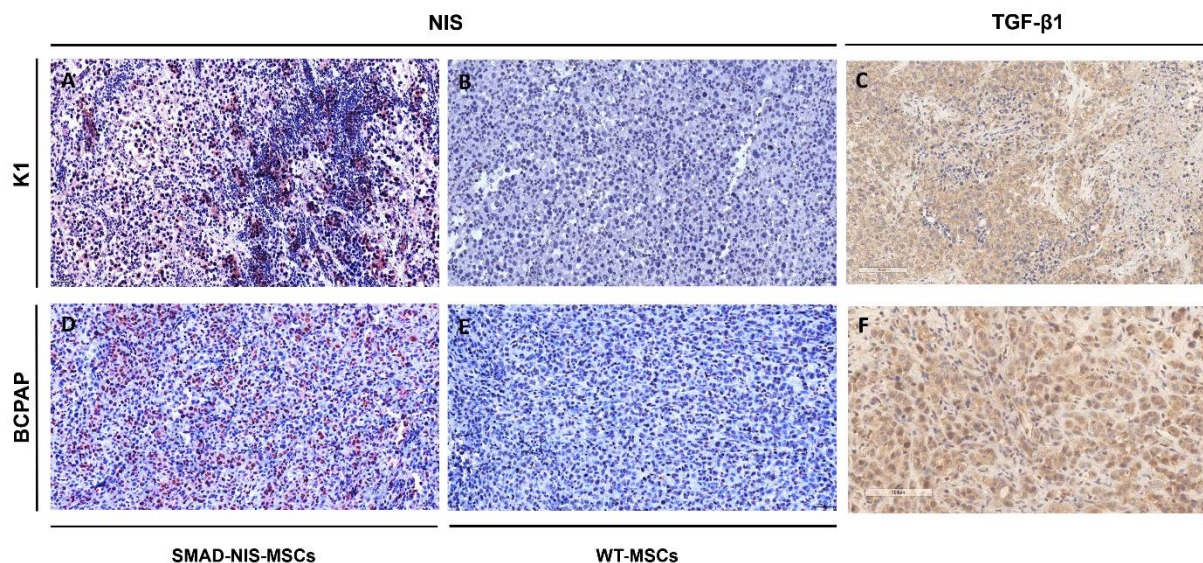
***Figure 8. Ex vivo tumoral NIS and TGF-β1 protein expression analysis.** NIS immunohistochemistry confirmed robust NIS protein expression in K1 **(A)** and BCPAP*

(D) tumors of mice that received systemic SMAD-NIS-MSCs application, while no NIS-specific immunoreactivity was detected after WT-MSCs injection (B, E). Abundant TGF-β1 protein expression was verified within the K1 (C) and BCPAP (F) tumors. One representative image is shown each (20× magnification).

## 8.8 *In vivo* ^{131}I therapy studies

Following the evaluation of NIS expression by ^{123}I-scintigraphy, an ^{131}I therapy trial was initiated in both BCPAP and K1 xenograft mice using SMAD-NIS-MSCs. After three SMAD-NIS-MSC applications in 48 h intervals, animals in the therapy group received a single ^{131}I injection (55.5 MBq). This cycle was repeated 24h after the first cycle. For the third therapy round, a single SMAD-NIS-MSC application was given followed by the last ^{131}I injection (55.5 MBq) (Fig 9A).

In mice harboring K1 xenografts tumors, the therapy group (SMAD-NIS-MSC + ^{131}I) showed a significant delay in tumor growth and a prolonged median survival time (28 days), whereas the mice in control groups received the WT-MSCs injection instead of SMAD-NIS-MSCs (WT-MSC + ^{131}I) revealed an exponential tumor growth and the median survival time was 24 days (Fig 9B, C). Control groups which received either SMAD-NIS-MSCs followed by saline treatment (NaCl) instead of ^{131}I (SMAD-NIS-MSC + NaCl) or saline only (NaCl + NaCl) both also showed continuous exponential tumor growth and significantly shorter median survival time (18 days) (Fig 9B, C).

The treatment of SMAD-NIS-MSCs followed by ^{131}I injection in BCPAP xenografts mice also resulted in a significant inhibition of the tumor growth as compared to the control groups (WT-MSCs + ^{131}I; SMAD-NIS-MSCs + NaCl; NaCl + NaCl) (Fig 9D). This treatment also resulted in a significantly prolonged survival as compared to the saline-control groups (SMAD-NIS-MSCs + NaCl; NaCl + NaCl). On day 54 after the start of therapy, although no statistical significance was observed between the survival of therapy group and WT-MSCs + ^{131}I group, only 25% of the mice that had received WT-

MSCs and ^{131}I treatment survived, whereas in the therapy group 66.7% mice were still

alive demonstrating a robust therapeutic effect (Fig 9E).
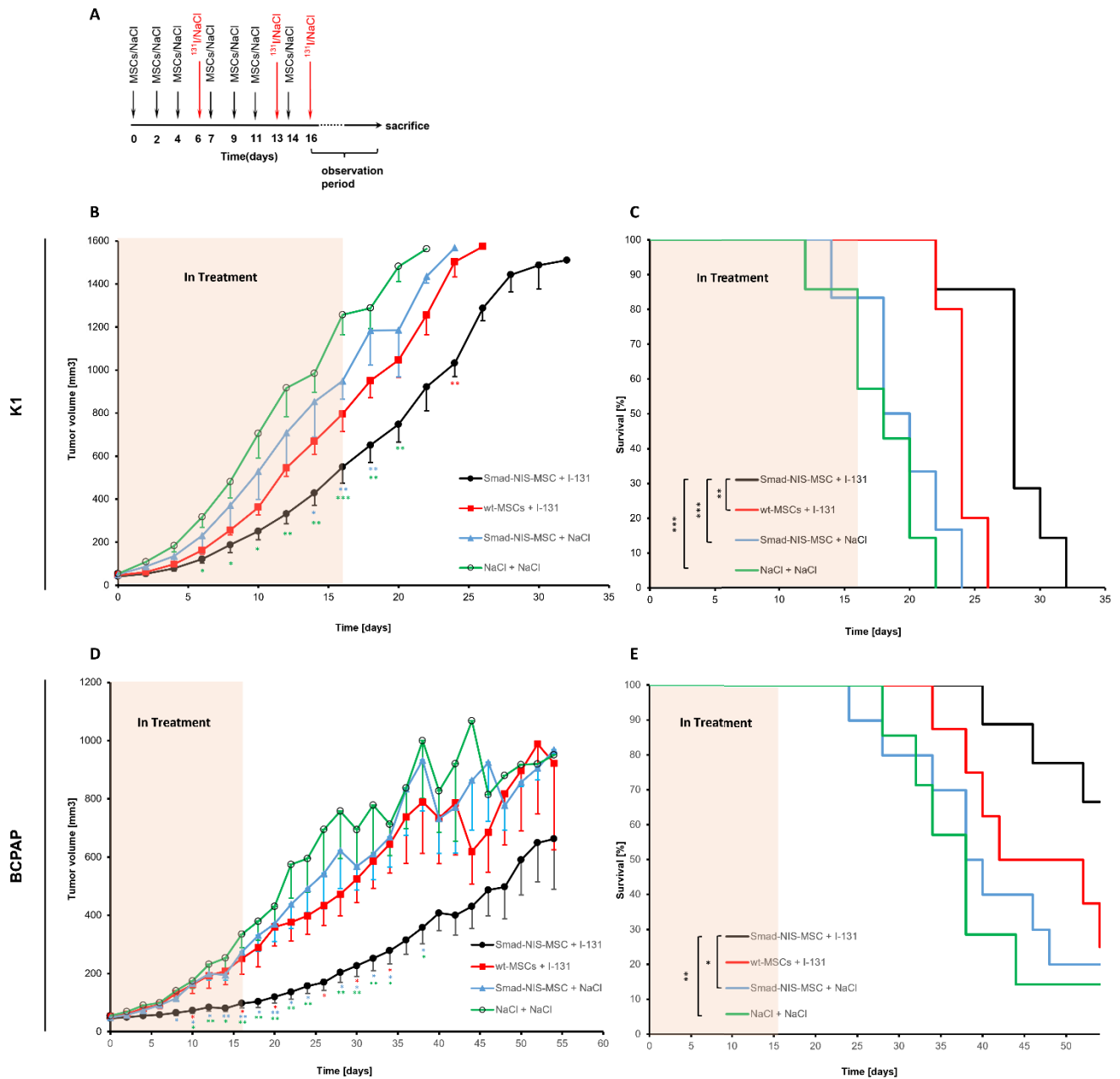
Figure 9. Therapeutic application of ^{131}I after systemic NIS gene transfer in K1 and BCPAP mouse model. *Mice harboring K1 and BCPAP xenograft tumors were treated with three consecutive i.v. SMAD-NIS-MSC injections (in 48h intervals) followed by an i.p. injection of 55.5 MBq ^{131}I. This cycle was repeated once. For the third cycle, a single SMAD-NIS-MSC was applied followed by ^{131}I **(A)**. Subcutaneous K1 mice treated with SMAD-NIS-MSCs and ^{131}I (SMAD-NIS-MSC + ^{131}I; n=7) resulted in a significant delay in tumor growth compared to the control groups receiving WT-MSCs and ^{131}I (WT-MSC + ^{131}I; n=5; **p<0.01), SMAD-NIS-MSCs and NaCl (SMAD-*

NIS-MSC + NaCl; n=6; *p<0.05; **p<0.01) or NaCl only (NaCl + NaCl; n=7; *p<0.05;
***p<0.01; ***p<0.001) **(B)**. It also led to an increased survival in the therapy group*
*(**p<0.01; ***p<0.001) **(C)**. As for therapy of mice harboring BCPAP tumors (SMAD-*
NIS-MSC + ^{131}I; n=9), tumor growth was significantly reduced and survival was
prolonged as compared to the controls (WT-MSC + ^{131}I: n=8; SMAD-NIS-MSC + NaCl:
*n=10; NaCl + NaCl: n=7; *p<0.05; **p<0.01) **(D, E)**. Data are represented as means*
values ± SEM for tumor growth and percentage for survival plots.

8.9 *Ex vivo* Ki67 and CD31 analysis

At the end of the therapy study, the tumors were dissected and stained for the cell
proliferation marker (Ki67; green) and marker for blood vessels (CD31; red) (Fig 10A,
D). Both K1 and BCPAP tumors treated with SMAD-NIS-MSCs and ^{131}I (SMAD-NIS-
MSCs + ^{131}I) showed a significantly lower proliferation index as compared to the control
groups (Fig 10B, E). The tumors in therapy group revealed a lower blood vessel density
of 1.05±0.13% (K1 xenograft tumors) and 1.54±0.12% (BCPAP xenograft tumors),
while the density was higher in control groups (Fig 10C, F).
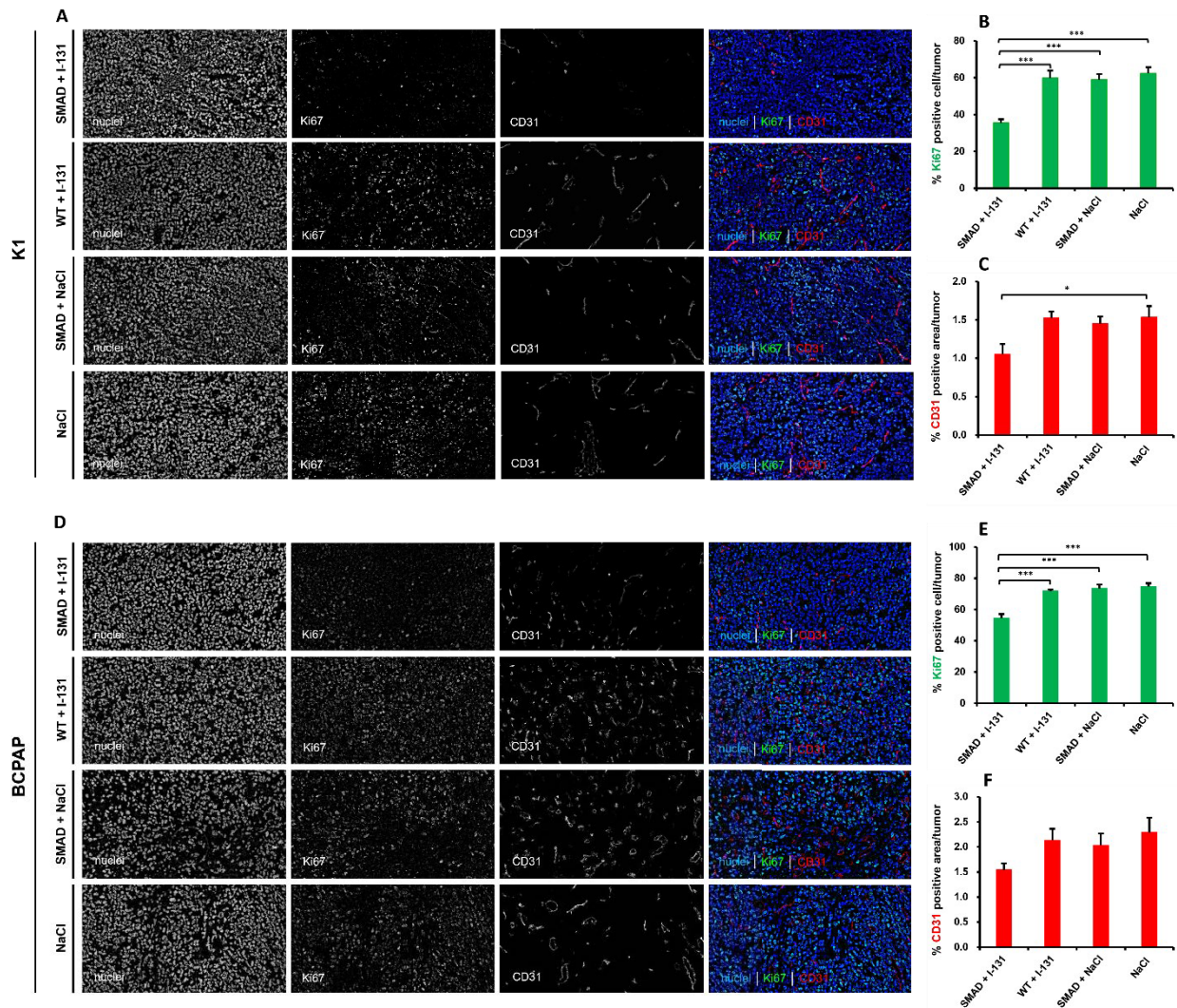
Figure 10. Ex vivo analysis of tumor cell proliferation and vascularization. *Tumor cell proliferation was assessed by Ki67 immunofluorescence staining (green) and blood vessel density by CD31 staining (red) on frozen tumor sections **(A, D)**. The staining revealed significantly decreased proliferation as well as reduced blood vessel density in K1 tumors **(B, C)** and BCPAP tumors **(E, F)** treated with SMAD-NIS-MSC followed by ^{131}I treatment as compared to the control tumors (mean ± SEM; *p<0.05, ***p<0.001). One representative image is shown each (20× magnification).*

9. Discussion

While the incidence of thyroid cancer has increased over the last 30 years, mortality levels have not changed significantly. In general, treatment with surgery in combination with radioiodine ablation and TSH suppression in a risk-stratified manner, is effective in most cases. Unfortunately, nearly 5% of patients present with locally advanced disease or distant metastases due to the development of radioiodine refractoriness, and significantly decreased patient survival [91]. The metastasized tumors show negligible ^{131}I uptake that is caused by loss of functional NIS expression or an impairment of NIS targeting to the membrane. Accumulating evidence now suggests that aberrant activation of the MAPK signaling pathway in differentiated thyroid cancer plays a central role in the reduction of NIS-mediated iodide accumulation [13]. An activating BRAFV600E mutation, a key activator of the MAPK pathway, is highly prevalent in recurrent RAI refractory PTC, and has been linked to the loss of RAI uptake and RAI responsiveness [92, 93]. In addition to the MAPK pathway, an autocrine loop involving TGF-β, which is also induced by BRAFV600E mutant thyroid tumors, was shown to act via SMAD to repress membrane-associated NIS expression [30, 94].

TGF-β signaling plays diverse tissue context-dependent roles in tumorigenesis: in premalignant cells TGF-β functions primarily as a tumor suppressor, while in advanced stages of cancer TGF-β signaling stimulates many tumors promoting processes, including proliferation, immune-suppression, epithelial-mesenchymal transition (EMT), cell migration, invasion, extracellular matrix remodeling, and metastasis [95]. TGF-β secretion has been demonstrated in normal and diseased thyroid follicular cells, and it has been implicated in the regulation of thyroid cell growth, differentiation and in gene regulation [30, 32]. In differentiated thyroid cancers, TGF-β is a potent inhibitor of iodide uptake and NIS expression. In addition to NIS, TGF-β acts as a suppressor of other thyroid-specific genes, such as thyroglobulin, thyroid peroxidase and the TSH receptor [96-98]. These data suggest a potential role of TGF-β as a candidate

therapeutic target for restoration of NIS expression in RAI refractory differentiated and dedifferentiated thyroid cancer. The re-induction of endogenous NIS expression allows the metastatic disease to be visualized by scintigraphy and become susceptible to radionuclide therapy. It is essential to find a safe and efficient way to deliver NIS to the tumors for the development of this concept towards clinical application.

Based on their tumor homing properties, mesenchymal stem cells (MSCs) represent a highly promising approach to deliver therapeutic genes into tumors. Our previous work has focused on systemic application of NIS to extrathyroidal tumors using mesenchymal stem cells as gene delivery vehicles [80-83, 86, 87]. These studies have extensively investigated the capacity of *NIS* gene transfer to induce radioiodine accumulation in tumors using MSCs as *NIS* transgene delivery vehicles. To help reduce potential side effects due to MSC recruitment to non-tumor tissues, MSCs have been engineered to express NIS under the control of gene promotors that are activated by tumor-related signals in order to enhance selectivity and the overall effectiveness of MSC-based *NIS* gene delivery. Our group has previously demonstrated the therapeutic efficiency of MSCs engineered with a TGF-β1-inducible SMAD-responsive promotor (SMAD-NIS-MSCs) for tumor-specific delivery of functional NIS to an HCC xenograft mouse model [84, 99]. Based in part on these previous results, we chose this approach and biology for MSC-mediated delivery of the *NIS* gene to RAI-refractory thyroid cancers. In the present study, high TGF-β1 expression was first confirmed in different thyroid cancer cell lines by qRT-PCR and ELISA. Using more physiologic tumor cell spheroids, the expression of the TGF-β1 protein or mRNA was found to be higher than that seen in monolayers, suggesting a higher level of TGF-β1 expression when tumor stroma is present. TGF-β1 expression within xenograft tumors derived from BCPAP and K1 cells was confirmed by TGF-β1 immunohistochemistry staining. It demonstrated higher TGF-β1 levels in BCPAP tumors as compared to K1 which was similar to what we have observed in qRT-PCR and ELISA analysis.

Stimulation of the SMAD-NIS-MSCs with conditioned medium from the tumor cell lines (K1, BHT101, BCPAP and MDA-T120) led to significant perchlorate-sensitive, NIS-

mediated radioiodine uptake showing significant stimulation of the TGF-β1/SMAD responsive promoter. Interestingly, all these cell lines are BRAF V600E positive. Despite lower TGF-β expression seen in some cell lines such as K1, high radioiodine uptake was induced in SMAD-NIS-MSC which might be due to the expression of other TGF-β superfamily factors such as activin [100, 101]. Importantly, the induced iodide uptake activity was fully inhibited by the TGF-β receptor inhibitor EW-7197, demonstrating that the induced NIS expression was under control of the TGF-β inducible SMAD-responsive promoter. In parallel experiments, SMAD-NIS-MSCs demonstrated a robust induction of radioiodine uptake activity upon co-culture with the tumor cells directly. These results illustrated the feasibility of this strategy for MSC-mediated induction of NIS gene expression in TGF-β1-rich thyroid carcinoma.

To test the potential directed migration of MSC towards the tumors and the role of TGF-β1 in this context, an *in vitro* migration assay was performed. The direct chemotaxis of MSCs towards the conditioned medium isolated from BCPAP and K1 cells confirmed the MSC homing to tumor signals that was inhibited in the presence of the TGF-β receptor inhibitor EW-7197 demonstrating a crucial role of TGF-β1 in this MSC tumor homing process. These experiments formed the basis for an *in vivo* approach to induce NIS-mediated iodide uptake in radioiodine refractory thyroid tumors using MSCs as gene delivery vehicles and the TGF-β1/SMAD responsive promoter to drive NIS expression in MSCs.

Based on these results an *in vivo* model of systemic MSC application in xenograft mouse models derived from BCPAP and K1 was established, ^{123}I-scintigraphy studies showed the recruitment of SMAD-NIS-MSCs into tumor environments and led to a significant perchlorate-sensitive, tumor-selective TGF-β1-driven iodide uptake in both models. As determined by gamma camera imaging, BCPAP xenograft tumors showed higher ^{123}I uptake than the K1 tumors, that confirms the previous observation in co-culture experiment that SMAD-NIS-MSCs accumulate more radioiodine when cultured with BCPAP than that with K1. NIS immunohistochemical staining demonstrated high NIS protein expression in tumors of mice injected with SMAD-NIS-MSCs. Importantly,

no SMAD-NIS-MSCs were found to be activated in non-target organs such as liver, lung, spleen and kidney, as was seen in our previous studies [84]. Adoptively applied MSCs not only show significant tumor tropism, but they potentially also home to normal tissues, such as the spleen or the lung [58]. Therefore, our approach using TGF-β1 to control the transgene expression reduced potential side-effects to non-tumor tissues.

Based on the *in vivo* and *ex vivo* imaging data, the therapeutic application of SMAD-NIS-MSCs and ^{131}I was conducted as a next step. In both models, we were able to demonstrate a significant reduction in tumor growth after the application of three cycles of SMAD-NIS-MSCs followed by ^{131}I, as compared to control groups. The K1 xenograft therapy group showed significantly prolonged survival as compared to control groups. A trend towards prolonged survival was seen in the BCPAP xenograft mouse therapy group but did not reach statistical significance as compared to the control mice (wild-type MSCs + [131]I). Staining for proliferating cells (Ki67) *ex vivo* confirmed reduced proliferation in the therapy mice. However, no significant difference was found between the groups for blood vessel density (CD31), except for the comparison between therapy group and saline group in K1 mice. An explanation might be the time point at which the tumors were resected. All the tumors were dissected and stained when the tumor exceeded the critical volume or started to ulcerate, when mice had to be sacrificed. Mice from the therapy group survived longer than the control mice, which allowed the recovery of the tumoral vascularization.

The goal of this study was to determine if it would be possible to restore responsiveness to RAI therapy in RAI refractory thyroid cancer by utilizing the high levels of TGF-β family ligands in the tumors to re-induce NIS-mediated RAI uptake using SMAD-NIS-MSCs. The TGF-β secreted by the tumors was found to enhance MSC recruitment, and to induce functional NIS expression via the TGF-β/SMAD pathway, and thus, allowed therapeutic ^{131}I accumulation in the tumors leading to destruction of tumor cells. The radioactive radiation of the tumor is thought to enhance an inflammatory response resulting in increased secretion of growth factors and chemokines, including TGF-β1 as shown by our previous study [102], thereby leading

to an enhanced recruitment of MSCs and higher induction of NIS expression [103, 104]. Thus, the TGF-β1-induced SMAD-promoter activity in MSCs results in enhancement of *NIS* transgene expression in the thyroid tumors due to repeated MSCs and radioiodine applications leading to a self-energizing cycle, which resulted in a robust therapeutic effect in the therapy study.

The results of this preclinical study strongly suggest the potential of using SMAD-NIS-MSCs to reinduce NIS expression in RAI refractory thyroid cancer. The findings identify a novel potential theranostic approach for the management of patients with metastasized radioiodine refractory thyroid cancer after thyroidectomy. The subcutaneous thyroid cancer xenografts used in the present study, which are the most commonly used due to the ease of handling and monitoring, rarely develop metastases and may not be fully representative of the characteristic behavior of human thyroid cancer metastasis [105]. In future studies, it would be advantageous to use a clinically more relevant mouse model of metastatic human thyroid cancer to more adequately investigate tumor homing and NIS expression of SMAD-NIS-MSCs in a preclinical model closer to the clinical situation.

10. Conclusion

RAI-refractory thyroid cancer remains a clinical challenge for postoperative management due to its unresponsiveness to radioiodine treatment. Our data demonstrated efficient tumoral recruitment of SMAD-NIS-MSCs and TGF-targeted NIS gene expression in subcutaneous thyroid cancer xenografts due to the overexpression of TGF-β1 in thyroid cancer, in particular BRAFV600E positive radioiodine refractory thyroid cancer. Combining the SMAD-NIS-MSC treatment with ^{131}I injection resulted in a reduction in tumor growth and prolonged survival. This proof-of-principle study suggests the feasibility of commandeering TGF-biology using TGF-β/SMAD-based signaling in the TGF-β1-rich tumor environments of radioiodine refractory DTC to re-establish functional NIS expression using engineered MSCs as therapy vehicles.

11. Acknowledgement

It was an important time of my life in this great university and I am very thankful to everyone who supported me during my thesis.

First of all, I would like to express my deepest gratitude to my supervisor Prof. Dr. Christine Spitzweg for letting me work on this exiting project in this great research group. Your constant support and supervisions help to walk me through all the periods of my doctoral study in this country. I could not get this thesis finished without your encouragement and guidance.

I would also thank my co-supervisor Prof. Dr. Peter J. Nelson for giving me the opportunity to study in Germany. Thank you for all the valuable advices and insightful opinions on research and thesis writing. Your supports give me a lot of confidence to finish my work here.

Many thanks to the whole Spitzweg lab for supporting me all these years. As the only man and foreigner in this lab, I really feel like I am in a warm family. Everyone is nice to me, and help me a lot with my work and life. Special thanks to Viktoria for all your support and cooperation of this project. Many thanks to Nathalie for cutting all my tissues, and giving me so much support of my life in Germany. I would like to thank Caro and Rebekka for all your help with my animal experiment. I cannot imagine how my therapy study would have gone without you. I would also thank Katy, Christina and Mariella for leading me into this scientific world. It's you that introduced the techniques and equipment to me. I really appreciate your patience. Furthermore, many thanks to our neighbor lab, for providing their microscope, scanner and so on.

Further I would like to thank the China Scholarship Council (CSC) for offering me the financial support, it's really of great help with my living abroad.

Additionally, I am grateful to all my friends here in Munich. You never made me feel lonely. It's my luck to meet you in my life.

Finally, I would like to show my deep gratitude to my family. You always understand me and support all the decisions I've made.

Love you all!

12. References

1.   Sung H, Ferlay J, Siegel RL, Laversanne M, Soerjomataram I, Jemal A, Bray F: Global Cancer Statistics 2020: GLOBOCAN Estimates of Incidence and Mortality Worldwide for 36 Cancers in 185 Countries. *CA Cancer J Clin* 2021, 71(3):209-249.

2.   Siegel RL, Miller KD, Jemal A: Cancer statistics, 2020. *CA Cancer J Clin* 2020, 70(1):7-30.

3.   Bray F, Ferlay J, Soerjomataram I, Siegel RL, Torre LA, Jemal A: Global cancer statistics 2018: GLOBOCAN estimates of incidence and mortality worldwide for 36 cancers in 185 countries. *CA Cancer J Clin* 2018, 68(6):394-424.

4.   Fagin JA, Wells SA, Jr.: Biologic and Clinical Perspectives on Thyroid Cancer. *N Engl J Med* 2016, 375(11):1054-1067.

5.   Hanahan D, Weinberg RA: The Hallmarks of Cancer. *Cell* 2000, 100(1):57-70.

6.   Hanahan D, Weinberg RA: Hallmarks of cancer: the next generation. *Cell* 2011, 144(5):646-674.

7.   Acquaviva G, Visani M, Repaci A, Rhoden KJ, de Biase D, Pession A, Giovanni T: Molecular pathology of thyroid tumours of follicular cells: a review of genetic alterations and their clinicopathological relevance. *Histopathology* 2018, 72(1):6-31.

8.   Nucera C, Lawler J, Parangi S: BRAF(V600E) and microenvironment in thyroid cancer: a functional link to drive cancer progression. *Cancer Res* 2011, 71(7):2417-2422.

9.   Xing M: BRAF mutation in papillary thyroid cancer: pathogenic role, molecular bases, and clinical implications. *Endocr Rev* 2007, 28(7):742-762.

10.   Xing M, Haugen BR, Schlumberger M: Progress in molecular-based management of differentiated thyroid cancer. *The Lancet* 2013, 381(9871):1058-1069.

11.   Fukahori M, Yoshida A, Hayashi H, Yoshihara M, Matsukuma S, Sakuma Y, Koizume S, Okamoto N, Kondo T, Masuda M *et al*: The associations between RAS

mutations and clinical characteristics in follicular thyroid tumors: new insights from a single center and a large patient cohort. *Thyroid* 2012, 22(7):683-689.

12.   Romei C, Ciampi R, Elisei R: A comprehensive overview of the role of the RET proto-oncogene in thyroid carcinoma. *Nat Rev Endocrinol* 2016, 12(4):192-202.

13.   Spitzweg C, Bible KC, Hofbauer LC, Morris JC: Advanced radioiodine-refractory differentiated thyroid cancer: the sodium iodide symporter and other emerging therapeutic targets. *Lancet Diabetes Endocrinol* 2014, 2(10):830-842.

14.   Riesco-Eizaguirre G, Santisteban P, De la Vieja A: The complex regulation of NIS expression and activity in thyroid and extrathyroidal tissues. *Endocr Relat Cancer* 2021, 28(10):T141-T165.

15.   Portulano C, Paroder-Belenitsky M, Carrasco N: The Na+/I- symporter (NIS): mechanism and medical impact. *Endocr Rev* 2014, 35(1):106-149.

16.   Hertz B: A tribute to Dr. Saul Hertz: The discovery of the medical uses of radioiodine. *World J Nucl Med* 2019, 18(1):8-12.

17.   Dai G, Levy O, Carrasco N: Cloning and characterization of the thyroid iodide transporter. *Nature* 1996, 379(6564):458-460.

18.   Penheiter AR, Russell SJ, Carlson SK: The sodium iodide symporter (NIS) as an imaging reporter for gene, viral, and cell-based therapies. *Curr Gene Ther* 2012, 12(1):33-47.

19.   Ravera S, Reyna-Neyra A, Ferrandino G, Amzel LM, Carrasco N: The Sodium/Iodide Symporter (NIS): Molecular Physiology and Preclinical and Clinical Applications. *Annu Rev Physiol* 2017, 79:261-289.

20.   Spitzweg C, Morris JC: Gene therapy for thyroid cancer: current status and future prospects. *Thyroid* 2004, 14(6):424-434.

21.   Spitzweg C, Morris JC: The sodium iodide symporter: its pathophysiological and therapeutic implications. *Clin Endocrinol (Oxf)* 2002, 57(5):559-574.

22.   Oh JM, Ahn BC: Molecular mechanisms of radioactive iodine refractoriness in differentiated thyroid cancer: Impaired sodium iodide symporter (NIS) expression owing to altered signaling pathway activity and intracellular localization of NIS. *Theranostics* 2021, 11(13):6251-6277.

23.   Kogai T, Brent GA: The sodium iodide symporter (NIS): regulation and approaches to targeting for cancer therapeutics. *Pharmacol Ther* 2012, 135(3):355-370.

24.   Aashiq M, Silverman DA, Na'ara S, Takahashi H, Amit M: Radioiodine-Refractory Thyroid Cancer: Molecular Basis of Redifferentiation Therapies, Management, and Novel Therapies. *Cancers (Basel)* 2019, 11(9).

25.   Cancer Genome Atlas Research N: Integrated genomic characterization of papillary thyroid carcinoma. *Cell* 2014, 159(3):676-690.

26.   Nagaraj NS, Datta PK: Targeting the transforming growth factor-beta signaling pathway in human cancer. *Expert Opin Investig Drugs* 2010, 19(1):77-91.

27.   Knauf JA, Sartor MA, Medvedovic M, Lundsmith E, Ryder M, Salzano M, Nikiforov YE, Giordano TJ, Ghossein RA, Fagin JA: Progression of BRAF-induced thyroid cancer is associated with epithelial-mesenchymal transition requiring concomitant MAP kinase and TGFbeta signaling. *Oncogene* 2011, 30(28):3153-3162.

28.   Papageorgis P, Stylianopoulos T: Role of TGFbeta in regulation of the tumor microenvironment and drug delivery (review). *Int J Oncol* 2015, 46(3):933-943.

29.   Batlle E, Massague J: Transforming Growth Factor-beta Signaling in Immunity and Cancer. *Immunity* 2019, 50(4):924-940.

30.   Riesco-Eizaguirre G, Rodriguez I, De la Vieja A, Costamagna E, Carrasco N, Nistal M, Santisteban P: The BRAFV600E oncogene induces transforming growth factor beta secretion leading to sodium iodide symporter repression and increased malignancy in thyroid cancer. *Cancer Res* 2009, 69(21):8317-8325.

31.　Vasko V, Espinosa AV, Scouten W, He H, Auer H, Liyanarachchi S, Larin A, Savchenko V, Francis GL, de la Chapelle A *et al*: Gene expression and functional evidence of epithelial-to-mesenchymal transition in papillary thyroid carcinoma invasion. *Proc Natl Acad Sci U S A* 2007, 104(8):2803-2808.

32.　Costamagna E, Garcia B, Santisteban P: The functional interaction between the paired domain transcription factor Pax8 and Smad3 is involved in transforming growth factor-beta repression of the sodium/iodide symporter gene. *J Biol Chem* 2004, 279(5):3439-3446.

33.　Lee MK, Pardoux C, Hall MC, Lee PS, Warburton D, Qing J, Smith SM, Derynck R: TGF-beta activates Erk MAP kinase signalling through direct phosphorylation of ShcA. *EMBO J* 2007, 26(17):3957-3967.

34.　Xing M: Genetic alterations in the phosphatidylinositol-3 kinase/Akt pathway in thyroid cancer. *Thyroid* 2010, 20(7):697-706.

35.　Garcia B, Santisteban P: PI3K is involved in the IGF-I inhibition of TSH-induced sodium/iodide symporter gene expression. *Mol Endocrinol* 2002, 16(2):342-352.

36.　Kogai T, Sajid-Crockett S, Newmarch LS, Liu YY, Brent GA: Phosphoinositide-3-kinase inhibition induces sodium/iodide symporter expression in rat thyroid cells and human papillary thyroid cancer cells. *J Endocrinol* 2008, 199(2):243-252.

37.　Tavares C, Eloy C, Melo M, Gaspar da Rocha A, Pestana A, Batista R, Bueno Ferreira L, Rios E, Sobrinho Simoes M, Soares P: mTOR Pathway in Papillary Thyroid Carcinoma: Different Contributions of mTORC1 and mTORC2 Complexes for Tumor Behavior and SLC5A5 mRNA Expression. *Int J Mol Sci* 2018, 19(5).

38.　Nicola JP, Nazar M, Mascanfroni ID, Pellizas CG, Masini-Repiso AM: NF-kappaB p65 subunit mediates lipopolysaccharide-induced Na(+)/I(-) symporter gene expression by involving functional interaction with the paired domain transcription factor Pax8. *Mol Endocrinol* 2010, 24(9):1846-1862.

39.   Faria M, Domingues R, Paixao F, Bugalho MJ, Matos P, Silva AL: TNFalpha-mediated activation of NF-kappaB downregulates sodium-iodide symporter expression in thyroid cells. *PLoS One* 2020, 15(2):e0228794.

40.   Shimura H, Haraguchi K, Miyazaki A, Endo T, Onaya T: Iodide uptake and experimental 131I therapy in transplanted undifferentiated thyroid cancer cells expressing the Na+/I- symporter gene. *Endocrinology* 1997, 138(10):4493-4496.

41.   Spitzweg C, O'Connor MK, Bergert ER, Tindall DJ, Young CY, Morris JC: Treatment of prostate cancer by radioiodine therapy after tissue-specific expression of the sodium iodide symporter. *Cancer Res* 2000, 60(22):6526-6530.

42.   Spitzweg C, Baker CH, Bergert ER, O'Connor MK, Morris JC: Image-guided radioiodide therapy of medullary thyroid cancer after carcinoembryonic antigen promoter-targeted sodium iodide symporter gene expression. *Hum Gene Ther* 2007, 18(10):916-924.

43.   Spitzweg C, Nelson PJ, Wagner E, Bartenstein P, Weber WA, Schwaiger M, Morris JC: The sodium iodide symporter (NIS): novel applications for radionuclide imaging and treatment. *Endocr Relat Cancer* 2021, 28(10):T193-T213.

44.   Trujillo MA, Oneal MJ, McDonough S, Qin R, Morris JC: A probasin promoter, conditionally replicating adenovirus that expresses the sodium iodide symporter (NIS) for radiovirotherapy of prostate cancer. *Gene Ther* 2010, 17(11):1325-1332.

45.   Klutz K, Willhauck MJ, Wunderlich N, Zach C, Anton M, Senekowitsch-Schmidtke R, Goke B, Spitzweg C: Sodium iodide symporter (NIS)-mediated radionuclide ((131)I, (188)Re) therapy of liver cancer after transcriptionally targeted intratumoral in vivo NIS gene delivery. *Hum Gene Ther* 2011, 22(11):1403-1412.

46.   Grunwald GK, Klutz K, Willhauck MJ, Schwenk N, Senekowitsch-Schmidtke R, Schwaiger M, Zach C, Goke B, Holm PS, Spitzweg C: Sodium iodide symporter (NIS)-mediated radiovirotherapy of hepatocellular cancer using a conditionally replicating adenovirus. *Gene Ther* 2013, 20(6):625-633.

47.   Dingli D, Peng KW, Harvey ME, Greipp PR, O'Connor MK, Cattaneo R, Morris JC, Russell SJ: Image-guided radiovirotherapy for multiple myeloma using a recombinant measles virus expressing the thyroidal sodium iodide symporter. *Blood* 2004, 103(5):1641-1646.

48.   Domingo-Musibay E, Allen C, Kurokawa C, Hardcastle JJ, Aderca I, Msaouel P, Bansal A, Jiang H, DeGrado TR, Galanis E: Measles Edmonston vaccine strain derivatives have potent oncolytic activity against osteosarcoma. *Cancer Gene Ther* 2014, 21(11):483-490.

49.   Mansfield DC, Kyula JN, Rosenfelder N, Chao-Chu J, Kramer-Marek G, Khan AA, Roulstone V, McLaughlin M, Melcher AA, Vile RG *et al*: Oncolytic vaccinia virus as a vector for therapeutic sodium iodide symporter gene therapy in prostate cancer. *Gene Ther* 2016, 23(4):357-368.

50.   Li H, Nakashima H, Decklever TD, Nace RA, Russell SJ: HSV-NIS, an oncolytic herpes simplex virus type 1 encoding human sodium iodide symporter for preclinical prostate cancer radiovirotherapy. *Cancer Gene Ther* 2013, 20(8):478-485.

51.   Liu YP, Wang J, Avanzato VA, Bakkum-Gamez JN, Russell SJ, Bell JC, Peng KW: Oncolytic vaccinia virotherapy for endometrial cancer. *Gynecol Oncol* 2014, 132(3):722-729.

52.   Pack DW, Hoffman AS, Pun S, Stayton PS: Design and development of polymers for gene delivery. *Nat Rev Drug Discov* 2005, 4(7):581-593.

53.   Klutz K, Russ V, Willhauck MJ, Wunderlich N, Zach C, Gildehaus FJ, Goke B, Wagner E, Ogris M, Spitzweg C: Targeted radioiodine therapy of neuroblastoma tumors following systemic nonviral delivery of the sodium iodide symporter gene. *Clin Cancer Res* 2009, 15(19):6079-6086.

54.   Klutz K, Willhauck MJ, Dohmen C, Wunderlich N, Knoop K, Zach C, Senekowitsch-Schmidtke R, Gildehaus FJ, Ziegler S, Furst S *et al*: Image-guided tumor-selective radioiodine therapy of liver cancer after systemic nonviral delivery of the sodium iodide symporter gene. *Hum Gene Ther* 2011, 22(12):1563-1574.

55.   Klutz K, Schaffert D, Willhauck MJ, Grunwald GK, Haase R, Wunderlich N, Zach C, Gildehaus FJ, Senekowitsch-Schmidtke R, Goke B *et al*: Epidermal growth factor receptor-targeted (131)I-therapy of liver cancer following systemic delivery of the sodium iodide symporter gene. *Mol Ther* 2011, 19(4):676-685.

56.   Schmohl KA, Dolp P, Schug C, Knoop K, Klutz K, Schwenk N, Bartenstein P, Nelson PJ, Ogris M, Wagner E *et al*: Reintroducing the Sodium-Iodide Symporter to Anaplastic Thyroid Carcinoma. *Thyroid* 2017, 27(12):1534-1543.

57.   Uchibori R, Tsukahara T, Ohmine K, Ozawa K: Cancer gene therapy using mesenchymal stem cells. *Int J Hematol* 2014, 99(4):377-382.

58.   Hagenhoff A, Bruns CJ, Zhao Y, von Luttichau I, Niess H, Spitzweg C, Nelson PJ: Harnessing mesenchymal stem cell homing as an anticancer therapy. *Expert Opin Biol Ther* 2016, 16(9):1079-1092.

59.   Chandler C, Liu T, Buckanovich R, Coffman LG: The double edge sword of fibrosis in cancer. *Transl Res* 2019, 209:55-67.

60.   Ding DC, Shyu WC, Lin SZ: Mesenchymal stem cells. *Cell Transplant* 2011, 20(1):5-14.

61.   Sun Z, Wang S, Zhao RC: The roles of mesenchymal stem cells in tumor inflammatory microenvironment. *J Hematol Oncol* 2014, 7:14.

62.   Melzer C, Yang Y, Hass R: Interaction of MSC with tumor cells. *Cell Commun Signal* 2016, 14(1):20.

63.   Studeny M, Marini FC, Dembinski JL, Zompetta C, Cabreira-Hansen M, Bekele BN, Champlin RE, Andreeff M: Mesenchymal stem cells: potential precursors for tumor stroma and targeted-delivery vehicles for anticancer agents. *J Natl Cancer Inst* 2004, 96(21):1593-1603.

64.   Nakamura K, Ito Y, Kawano Y, Kurozumi K, Kobune M, Tsuda H, Bizen A, Honmou O, Niitsu Y, Hamada H: Antitumor effect of genetically engineered mesenchymal stem cells in a rat glioma model. *Gene Ther* 2004, 11(14):1155-1164.

65. Elzaouk L, Moelling K, Pavlovic J: Anti-tumor activity of mesenchymal stem cells producing IL-12 in a mouse melanoma model. *Exp Dermatol* 2006, 15(11):865-874.

66. Xin H, Kanehira M, Mizuguchi H, Hayakawa T, Kikuchi T, Nukiwa T, Saijo Y: Targeted delivery of CX3CL1 to multiple lung tumors by mesenchymal stem cells. *Stem Cells* 2007, 25(7):1618-1626.

67. Grisendi G, Bussolari R, Cafarelli L, Petak I, Rasini V, Veronesi E, De Santis G, Spano C, Tagliazzucchi M, Barti-Juhasz H *et al*: Adipose-derived mesenchymal stem cells as stable source of tumor necrosis factor-related apoptosis-inducing ligand delivery for cancer therapy. *Cancer Res* 2010, 70(9):3718-3729.

68. Loebinger MR, Eddaoudi A, Davies D, Janes SM: Mesenchymal stem cell delivery of TRAIL can eliminate metastatic cancer. *Cancer Res* 2009, 69(10):4134-4142.

69. Zischek C, Niess H, Ischenko I, Conrad C, Huss R, Jauch KW, Nelson PJ, Bruns C: Targeting tumor stroma using engineered mesenchymal stem cells reduces the growth of pancreatic carcinoma. *Ann Surg* 2009, 250(5):747-753.

70. Conrad C, Husemann Y, Niess H, von Luettichau I, Huss R, Bauer C, Jauch KW, Klein CA, Bruns C, Nelson PJ: Linking transgene expression of engineered mesenchymal stem cells and angiopoietin-1-induced differentiation to target cancer angiogenesis. *Ann Surg* 2011, 253(3):566-571.

71. Niess H, Bao Q, Conrad C, Zischek C, Notohamiprodjo M, Schwab F, Schwarz B, Huss R, Jauch KW, Nelson PJ *et al*: Selective targeting of genetically engineered mesenchymal stem cells to tumor stroma microenvironments using tissue-specific suicide gene expression suppresses growth of hepatocellular carcinoma. *Ann Surg* 2011, 254(5):767-774; discussion 774-765.

72. von Einem JC, Guenther C, Volk HD, Grutz G, Hirsch D, Salat C, Stoetzer O, Nelson PJ, Michl M, Modest DP *et al*: Treatment of advanced gastrointestinal cancer with genetically modified autologous mesenchymal stem cells: Results from the phase 1/2 TREAT-ME-1 trial. *Int J Cancer* 2019, 145(6):1538-1546.

73.   Komarova S, Kawakami Y, Stoff-Khalili MA, Curiel DT, Pereboeva L: Mesenchymal progenitor cells as cellular vehicles for delivery of oncolytic adenoviruses. *Mol Cancer Ther* 2006, 5(3):755-766.

74.   Stoff-Khalili MA, Rivera AA, Mathis JM, Banerjee NS, Moon AS, Hess A, Rocconi RP, Numnum TM, Everts M, Chow LT *et al*: Mesenchymal stem cells as a vehicle for targeted delivery of CRAds to lung metastases of breast carcinoma. *Breast Cancer Res Treat* 2007, 105(2):157-167.

75.   Yong RL, Shinojima N, Fueyo J, Gumin J, Vecil GG, Marini FC, Bogler O, Andreeff M, Lang FF: Human bone marrow-derived mesenchymal stem cells for intravascular delivery of oncolytic adenovirus Delta24-RGD to human gliomas. *Cancer Res* 2009, 69(23):8932-8940.

76.   Yao S, Li X, Liu J, Sun Y, Wang Z, Jiang Y: Maximized nanodrug-loaded mesenchymal stem cells by a dual drug-loaded mode for the systemic treatment of metastatic lung cancer. *Drug Deliv* 2017, 24(1):1372-1383.

77.   Takayama Y, Kusamori K, Tsukimori C, Shimizu Y, Hayashi M, Kiyama I, Katsumi H, Sakane T, Yamamoto A, Nishikawa M: Anticancer drug-loaded mesenchymal stem cells for targeted cancer therapy. *J Control Release* 2021, 329:1090-1101.

78.   Layek B, Sadhukha T, Panyam J, Prabha S: Nano-Engineered Mesenchymal Stem Cells Increase Therapeutic Efficacy of Anticancer Drug Through True Active Tumor Targeting. *Mol Cancer Ther* 2018, 17(6):1196-1206.

79.   Wang X, Chen H, Zeng X, Guo W, Jin Y, Wang S, Tian R, Han Y, Guo L, Han J *et al*: Efficient lung cancer-targeted drug delivery via a nanoparticle/MSC system. *Acta Pharm Sin B* 2019, 9(1):167-176.

80.   Knoop K, Kolokythas M, Klutz K, Willhauck MJ, Wunderlich N, Draganovici D, Zach C, Gildehaus FJ, Boning G, Goke B *et al*: Image-guided, tumor stroma-targeted 131I therapy of hepatocellular cancer after systemic mesenchymal stem cell-mediated NIS gene delivery. *Mol Ther* 2011, 19(9):1704-1713.

81.   Knoop K, Schwenk N, Schmohl K, Muller A, Zach C, Cyran C, Carlsen J, Boning G, Bartenstein P, Goke B *et al*: Mesenchymal stem cell-mediated, tumor stroma-targeted radioiodine therapy of metastatic colon cancer using the sodium iodide symporter as theranostic gene. *J Nucl Med* 2015, 56(4):600-606.

82.   Knoop K, Schwenk N, Dolp P, Willhauck MJ, Zischek C, Zach C, Hacker M, Goke B, Wagner E, Nelson PJ *et al*: Stromal targeting of sodium iodide symporter using mesenchymal stem cells allows enhanced imaging and therapy of hepatocellular carcinoma. *Hum Gene Ther* 2013, 24(3):306-316.

83.   Muller AM, Schmohl KA, Knoop K, Schug C, Urnauer S, Hagenhoff A, Clevert DA, Ingrisch M, Niess H, Carlsen J *et al*: Hypoxia-targeted 131I therapy of hepatocellular cancer after systemic mesenchymal stem cell-mediated sodium iodide symporter gene delivery. *Oncotarget* 2016, 7(34):54795-54810.

84.   Schug C, Urnauer S, Jaeckel C, Schmohl KA, Tutter M, Steiger K, Schwenk N, Schwaiger M, Wagner E, Nelson PJ *et al*: TGFB1-driven mesenchymal stem cell-mediated NIS gene transfer. *Endocr Relat Cancer* 2019, 26(1):89-101.

85.   Schmohl KA, Mueller AM, Dohmann M, Spellerberg R, Urnauer S, Schwenk N, Ziegler SI, Bartenstein P, Nelson PJ, Spitzweg C: Integrin alphavbeta3-Mediated Effects of Thyroid Hormones on Mesenchymal Stem Cells in Tumor Angiogenesis. *Thyroid* 2019, 29(12):1843-1857.

86.   Tutter M, Schug C, Schmohl KA, Urnauer S, Schwenk N, Petrini M, Lokerse WJM, Zach C, Ziegler S, Bartenstein P *et al*: Effective control of tumor growth through spatial and temporal control of theranostic sodium iodide symporter (NIS) gene expression using a heat-inducible gene promoter in engineered mesenchymal stem cells. *Theranostics* 2020, 10(10):4490-4506.

87.   Tutter M, Schug C, Schmohl KA, Urnauer S, Kitzberger C, Schwenk N, Petrini M, Zach C, Ziegler S, Bartenstein P *et al*: Regional Hyperthermia Enhances Mesenchymal Stem Cell Recruitment to Tumor Stroma: Implications for Mesenchymal Stem Cell-Based Tumor Therapy. *Mol Ther* 2021, 29(2):788-803.

88. Spitzweg C, Zhang S, Bergert ER, Castro MR, McIver B, Heufelder AE, Tindall DJ, Young CY, Morris JC: Prostate-specific antigen (PSA) promoter-driven androgen-inducible expression of sodium iodide symporter in prostate cancer cell lines. *Cancer Res* 1999, 59(9):2136-2141.

89. Schmohl KA, Muller AM, Wechselberger A, Ruhland S, Salb N, Schwenk N, Heuer H, Carlsen J, Goke B, Nelson PJ *et al*: Thyroid hormones and tetrac: new regulators of tumour stroma formation via integrin alphavbeta3. *Endocr Relat Cancer* 2015, 22(6):941-952.

90. Urnauer S, Morys S, Krhac Levacic A, Muller AM, Schug C, Schmohl KA, Schwenk N, Zach C, Carlsen J, Bartenstein P *et al*: Sequence-defined cMET/HGFR-targeted Polymers as Gene Delivery Vehicles for the Theranostic Sodium Iodide Symporter (NIS) Gene. *Mol Ther* 2016, 24(8):1395-1404.

91. Kirtane K, Roth MY: Emerging Therapies for Radioactive Iodine Refractory Thyroid Cancer. *Curr Treat Options Oncol* 2020, 21(3):18.

92. Elisei R, Ugolini C, Viola D, Lupi C, Biagini A, Giannini R, Romei C, Miccoli P, Pinchera A, Basolo F: BRAF(V600E) mutation and outcome of patients with papillary thyroid carcinoma: a 15-year median follow-up study. *J Clin Endocrinol Metab* 2008, 93(10):3943-3949.

93. Chakravarty D, Santos E, Ryder M, Knauf JA, Liao XH, West BL, Bollag G, Kolesnick R, Thin TH, Rosen N *et al*: Small-molecule MAPK inhibitors restore radioiodine incorporation in mouse thyroid cancers with conditional BRAF activation. *J Clin Invest* 2011, 121(12):4700-4711.

94. Riesco-Eizaguirre G, Gutierrez-Martinez P, Garcia-Cabezas MA, Nistal M, Santisteban P: The oncogene BRAF V600E is associated with a high risk of recurrence and less differentiated papillary thyroid carcinoma due to the impairment of Na+/I-targeting to the membrane. *Endocr Relat Cancer* 2006, 13(1):257-269.

95. Bierie B, Moses HL: Tumour microenvironment: TGFbeta: the molecular Jekyll and Hyde of cancer. *Nat Rev Cancer* 2006, 6(7):506-520.

96.	Kang HC, Ohmori M, Harii N, Endo T, Onaya T: Pax-8 is essential for regulation of the thyroglobulin gene by transforming growth factor-beta1. *Endocrinology* 2001, 142(1):267-275.

97.	Taton M, Lamy F, Roger PP, Dumont JE: General inhibition by transforming growth factor beta 1 of thyrotropin and cAMP responses in human thyroid cells in primary culture. *Mol Cell Endocrinol* 1993, 95(1-2):13-21.

98.	Kawaguchi A, Ikeda M, Endo T, Kogai T, Miyazaki A, Onaya T: Transforming growth factor-beta1 suppresses thyrotropin-induced Na+/I- symporter messenger RNA and protein levels in FRTL-5 rat thyroid cells. *Thyroid* 1997, 7(5):789-794.

99.	Schug C, Kitzberger C, Sievert W, Spellerberg R, Tutter M, Schmohl KA, Eberlein B, Biedermann T, Steiger K, Zach C *et al*: Radiation-Induced Amplification of TGFB1-Induced Mesenchymal Stem Cell-Mediated Sodium Iodide Symporter (NIS) Gene (131)I Therapy. *Clin Cancer Res* 2019, 25(19):5997-6008.

100.	Kimura ET, Matsuo SE, Ricarte-Filho JC: [TGFbeta, activin and SMAD signalling in thyroid cancer]. *Arq Bras Endocrinol Metabol* 2007, 51(5):683-689.

101.	Schulte KM, Jonas C, Krebs R, Roher HD: Activin A and activin receptors in thyroid cancer. *Thyroid* 2001, 11(1):3-14.

102.	Schug C, Sievert W, Urnauer S, Muller AM, Schmohl KA, Wechselberger A, Schwenk N, Lauber K, Schwaiger M, Multhoff G *et al*: External Beam Radiation Therapy Enhances Mesenchymal Stem Cell-Mediated Sodium-Iodide Symporter Gene Delivery. *Hum Gene Ther* 2018, 29(11):1287-1300.

103.	Klopp AH, Spaeth EL, Dembinski JL, Woodward WA, Munshi A, Meyn RE, Cox JD, Andreeff M, Marini FC: Tumor irradiation increases the recruitment of circulating mesenchymal stem cells into the tumor microenvironment. *Cancer Res* 2007, 67(24):11687-11695.

104.	Zielske SP, Livant DL, Lawrence TS: Radiation increases invasion of gene-modified mesenchymal stem cells into tumors. *Int J Radiat Oncol Biol Phys* 2009, 75(3):843-853.

105. Lwin TM, Hoffman RM, Bouvet M: Advantages of patient-derived orthotopic mouse models and genetic reporters for developing fluorescence-guided surgery. *J Surg Oncol* 2018, 118(2):253-264.